Chapter 3
Waves

3-1. Introduction

Waves are the dominant force controlling littoral processes on open coasts. Determination of appropriate wave conditions is necessary before estimates of currents and sediment transport can be undertaken. Waves are the major factor in determining the geometry and composition of beaches and significantly enter into the planning and design of coastal structures. Waves generally derive their energy from storms over the open ocean. A significant amount of this energy may be dissipated before the waves reach the design site. An understanding of surface waves must precede a description of water motions in the nearshore. This chapter provides information necessary for the reader to assimilate and apply guidance presented in succeeding chapters; it is not intended to be a complete reference on waves. Additional information concerning obtaining, interpreting, and applying wave and water level information can be found in EM 1110-2-1414. This chapter defines terms and explains concepts used for littoral transport estimates, presents an overview of linear wave theory, discusses methods for determining deep water wave conditions, and explains propagation of these deep water waves to the nearshore. Chapter 2 of the Shore Protection Manual (SPM) (1984) provides a thorough introduction to the linear theory of surface water waves.

3-2. Description of Waves

a. Wave energy. Energy in the nearshore zone occurs over a broad range of frequencies. An approximate distribution of this energy is shown in Figure 3-1. The waves addressed in this chapter fall within the gravity wave band. However, studies have suggested that infragravity waves also play a significant role in littoral processes (e.g., Komar and Holman 1986). A number of terms commonly associated with the description of surface water waves are defined in Figure 3-2.

b. Linear wave theory.

(1) Waves in the ocean often appear confused, with constantly changing crests and troughs on the water surface. This is particularly true when waves are under the influence of the wind. However, it is often assumed that waves are simple periodic, so that each wave is exactly the same as all others. Simple periodic waves may either be linear or nonlinear. There are a number of periodic wave theories, but the most commonly employed is linear wave theory (LWT), also known as Airy wave theory. Regions of validity for various wave theories are shown in Figure 3-3. In LWT, the free surface is assumed to be a simple sinusoid and the amplitude of the crest a_c equals the amplitude of the trough a_t. Linearized free surface boundary conditions are applied at the still-water level (SWL), also referred to as the mean water line (MWL), rather than at the actual surface. For this condition to be satisfied, the wave height to wavelength ratio must be very small. In spite of these restrictions, LWT is often applied for large waves with reasonable success in littoral processes descriptions. Sinusoidal waves are characterized by the wave height H, wave period T, and water depth d.

(2) The wavelength is related to the water depth and wave period through the dispersion equation. This is a transcendental relationship and solutions may not be obtained explicitly for arbitrary water depths. Therefore, it is common to consider the deep and shallow water limits in the hyperbolic tangent function to develop simplifications. These are summarized in Table 3-1. Solutions to the dispersion equation for arbitrary depths are tabulated in Appendix C in the Shore Protection Manual (1984). Solutions may also be easily determined on microcomputers using the half-interval method, Newton-Raphson or Padé approximates. A FORTRAN subroutine based on Padé approximates (Hunt 1979) is given in Table 3-2. A simple approximation which provides reasonable accuracy in shallow and intermediate water depths is

$$L = \left(2\pi d L_0\right)^{\frac{1}{2}} \left(1 - \frac{\pi d}{3L_0}\right) \tag{3-1}$$

in which L is the wave length, π = 3.14159..., and L_0 is the deep water wavelength given in Table 3-1. The relative error for this relationship is less than 2% for $d/L_0 < 0.3$.

(3) As waves approach the nearshore, the crests become higher and steeper, and the troughs become longer and flatter. The assumptions of LWT are no longer valid. Nonlinear wave theories provide a better description of the waves. The nonlinearities are important in nearshore processes. For example, steep waves exert a larger on-shore bottom stress which is significant in the development of an equilibrium beach profile.

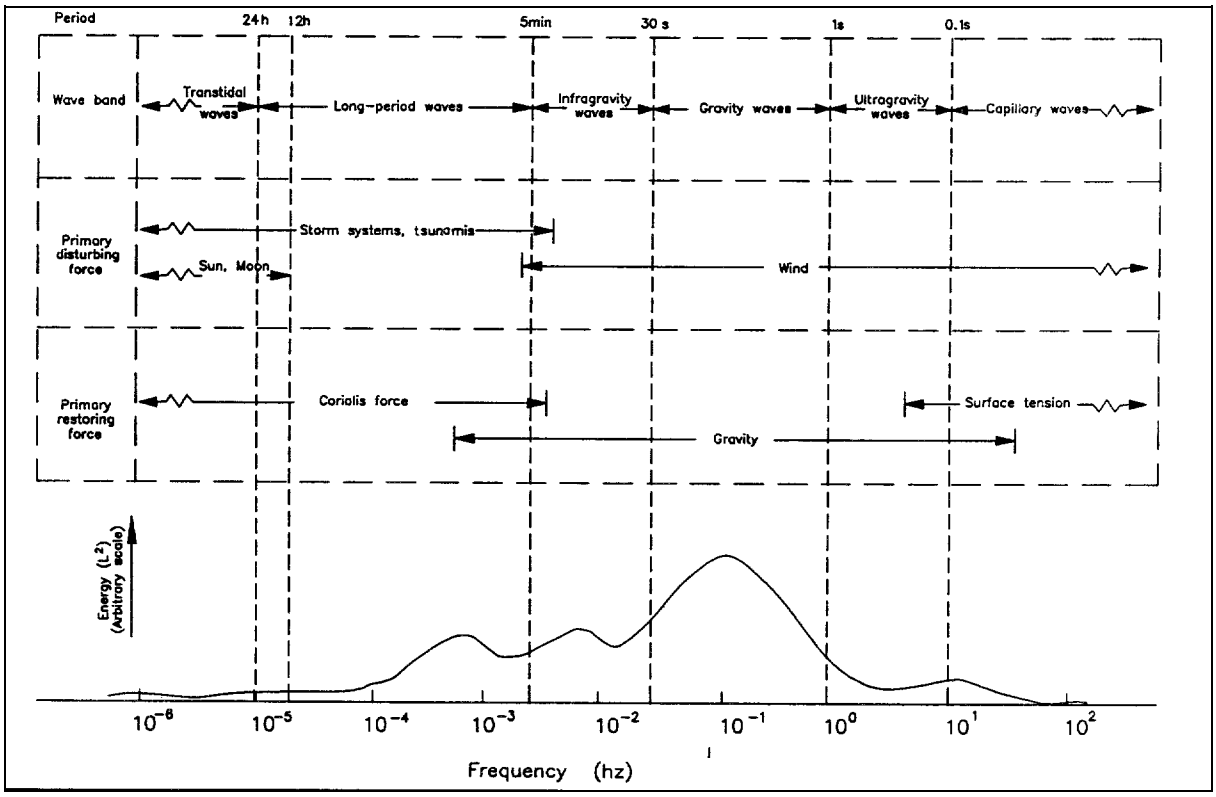

Figure 3-1. Approximate distribution of ocean surface wave energy (after Kinsman 1965)

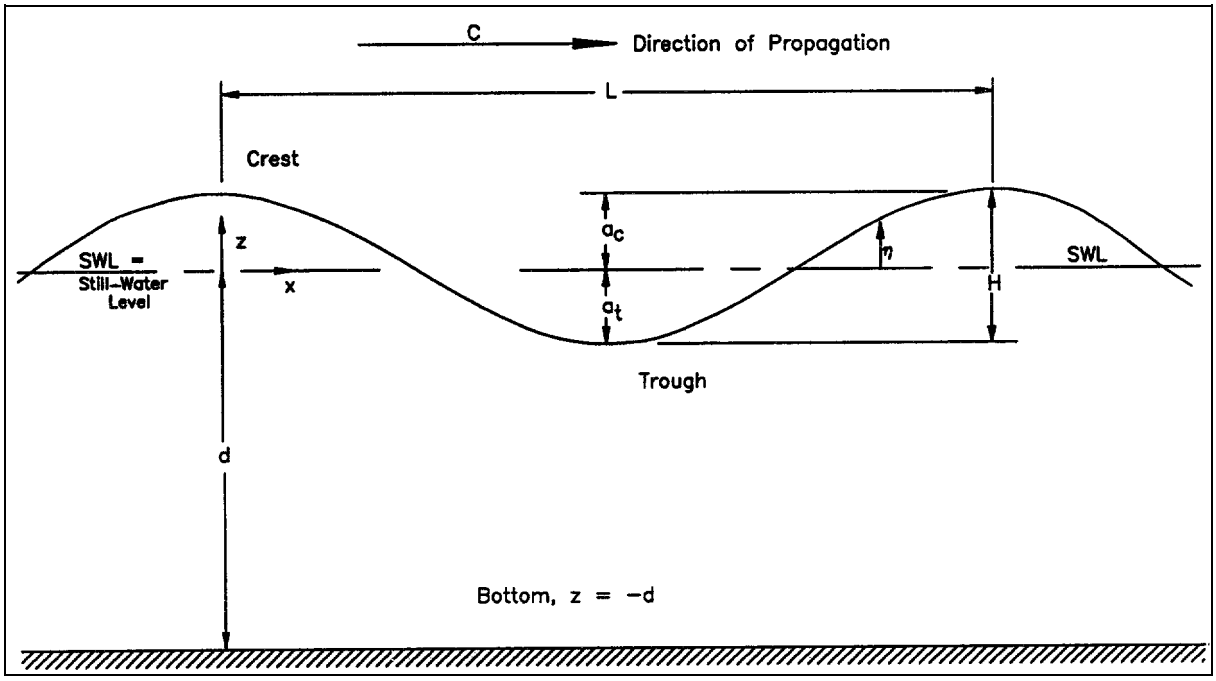

Figure 3-2. Definitions of surface waves

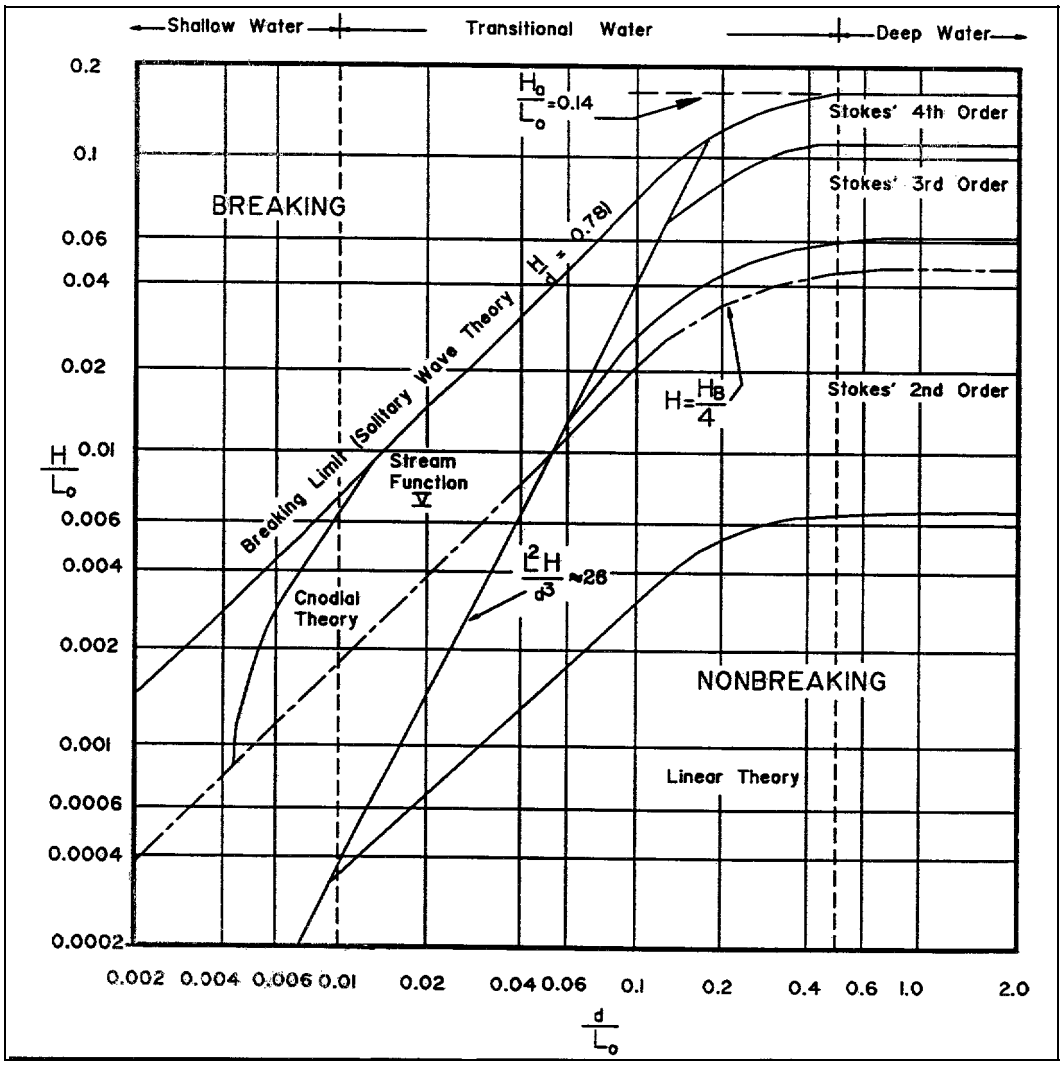

Figure 3-3. Regions of validity for various wave theories (after LeMehaute 1969)

In spite of this, most models for estimating longshore currents and sediment transport are based on LWT. In fact, many of the published models use shallow water LWT. Therefore, no discussion of nonlinear waves is given. Appendix A provides a list of references which address this topic. A review of nonlinear wave theories is given by Dean and Dalrymple (1983).

c. Short term wave statistics.

(1) Wave heights measured over a duration of several hours will show a variation, even if the spectrum does not change with time. If the waves have a narrow banded spectrum (small variation in wave period), then the wave heights are Rayleigh distributed (Longuet-Higgins 1952). The Rayleigh distribution is given by

$$P(H) = 1 - \exp\left(\frac{-H^2}{H_{rms}^2}\right) \tag{3-2}$$

where $P(H)$ is the probability of wave height H occurring, and H_{rms} is the root mean square *(rms)* wave height defined by

Table 3-1
Linear Wave Theory Relationships

		Shallow Water ($d/L < 1/25$)	Intermediate Water ($1/25 < d/L < 1/2$)	Deep Water ($d/L > 1/2$)
Wave profile	^{n}	same as $\rightarrow$	$\frac{H}{2}\cos\Theta$	$\leftarrow$ same as
Wavelength	L	$(gd)^{1/2}\ T$	$\frac{gT^2}{2\pi}\tanh kd$	$\frac{gT^2}{2\pi}$
Wave speed	C	$(gd)^{1/2}$	$\frac{gT}{2\pi}\tanh kd$	$\frac{gT}{2\pi}$
Group speed	C_g	$(gd)^{1/2}$	$1 + \frac{2kd}{\sinh 2kd}\ \frac{C}{2}$	$\frac{gT}{4\pi}$
Horizontal component of particle velocity	u	$\frac{H}{2}\ (g/d)^{1/2}\cos\Theta$	$\frac{H}{2}\frac{gk}{\omega}\frac{\cosh k(d+z)}{\cosh kd}\cos\Theta$	$\frac{\pi H}{T}e^{ks}\cos\Theta$
Vertical component of particle velocity	w	$\frac{H\pi}{T}(1+z/d)\sin\Theta$	$\frac{H}{2}\frac{gk}{\omega}\frac{\sinh k(d+z)}{\cosh kd}\sin\Theta$	$\frac{\pi H}{T}e^{kz}\sin\Theta$
Subsurface pressure	p	$\rho g(n-z)$	$\rho g\ \ n\ \frac{\cosh k(d+z)}{\cosh kd} - z$	$\rho g(n\,e^{kz} - z)$

Note:

Θ = phase angle = $2\pi\ \frac{X}{L} - \frac{t}{T}$

k = wave number = $\frac{2\pi}{L}$

ω = frequency (in radians) = $\frac{2\pi}{T}$

Table 3-2
FORTRAN Subroutine to Estimate Wavelength Using Padé Approximates (Hunt 1979)

```
      SUBROUTINE PADÉ (DEPTH, PERIOD, GRAVITY, LENGTH)
C     This subroutine gives a solution to the linear wave theory
C     dispersion equation using Pade' approximates.
C
C     DEPTH                STILL WATER DEPTH
C     PERIOD               WAVE PERIOD
C     GRAVITY              ACCELERATION DUE TO GRAVITY
C     LENGTH               WAVELENGTH
      REAL LENGTH, C(6)

      DATA C/0.666, 0.355, 0.1608465608, 0.0632098765,
                           0.0217540484, 0.0065407983/

      PI=4.*ATAN(1.)
      Y=DEPTH*(2.*PI/PERIOD)**2/GRAVITY
      SUM=0.
      DO 100 I=1,6
100   SUM=SUM+C(I)*Y**I
      LENGTH=2.*PI*DEPTH/SQRT(Y**2+Y/(1.+SUM))
      RETURN
      END
```

$$H_{rms} = \left(\frac{1}{N} \sum_{n=1}^{N} H_n^2 \right)^{\frac{1}{2}} \quad (3\text{-}3)$$

H_{rms} characterizes the distribution of the waves. However, other statistically representative waves are often used in engineering practice. The average of the highest n waves in the distribution is termed $H_{1/n}$. The case where $n = 3$ is termed the significant wave height and approximately corresponds to the wave height that a trained observer would visually determine. $H_{1/3}$ is often denoted as H_s. The relationship between H_{rms} and other statistically representative waves is summarized in Table 3-3.

Table 3-3
Statistically Representative Waves Based on Rayleigh Wave Height Relationships

Wave Height	Notation	H/H_{rms}
Mode	--	0.707
Median	--	0.833
Mean	$\overline{H} = H_1$	0.886
Root-mean-square	H_{rms}	1.000
Significant	$H_s = H_{1/3}$	1.416
Average of tenth-highest waves	$H_{1/10}$	1.800
Average of hundredth-highest waves	$H_{1/100}$	2.359

(2) The largest wave H_{max} in a wave record is approximately (Goda 1985)

$$\frac{H_{max}}{H_s} = \left(\frac{\ln N}{2} \right)^{\frac{1}{2}} + e \, (8 \ln N)^{\frac{1}{2}} \quad (3\text{-}4)$$

in which N is the number of waves and e is Euler's constant ($e \sim 0.5722$). The Rayleigh distribution is particularly suited to a narrow banded spectrum, so the peak frequency f_p may be used to determine the number of waves in the record. The peak frequency is the frequency corresponding to the maximum energy in the spectrum. Assuming the waves are stationary (i.e., the wave spectrum does not change with time), then $N = D/T_p$ where D is the duration of the record or storm and T_p is the peak period. The maximum expected wave height is shown in Figure 3-4 for different peak periods for a fully developed spectrum having a Rayleigh distribution of heights. The maximum expected wave height may be useful for estimating extreme runup, overtopping, and wave forces.

(3) Waves are usually recorded as a digital time series of the free surface elevation. There are two common techniques for recovering the significant wave height and period from these records, zero downcrossing and spectral analysis.

(4) The significant wave height can be estimated from a digital record by direct computation of $H_{1/3}$. Individual waves are between successive points where the free surface passes down through the mean elevation. The height for each of these zero downcrossing waves is then determined. These heights are ranked and the average of the highest one-third is $H_{1/3}$. The significant wave period can be determined in a similar manner. The mean period is calculated as the average of all of the wave periods.

(5) In the spectral approach, the significant wave height in deep water is defined as four times the standard deviation of the record of sea surface elevations. The significant wave height determined in this manner is the zero moment wave height, denoted as H_{m0}, to clearly identify that it was obtained by the spectral approach. The exact value of H_{m0} depends on wave steepness and relative depth as indicated in Figure 3-5. In the spectral approach, the significant wave period T_p is often taken as the period corresponding with the peak energy, and the finite depth wavelength of waves at the spectral peak is denoted as L_p. The mean period is calculated from the square root of the ratio of the zeroeth to the second moment of the spectrum.

(6) Both of these methods provide reasonable results and both are commonly used. Since the two approaches yield slightly different results, it should be made clear which approach is being used to estimate the significant wave height, significant period, and mean period.

d. Long-term wave statistics. Extreme wave heights are an important parameter in many coastal designs. Often the extreme wave heights are limited by the water depth. For deeper water or low energy sites, extreme values are usually described in terms of significant wave height as a function of the return period. Extreme values of other height statistics, such as $H_{1/10}$, can be

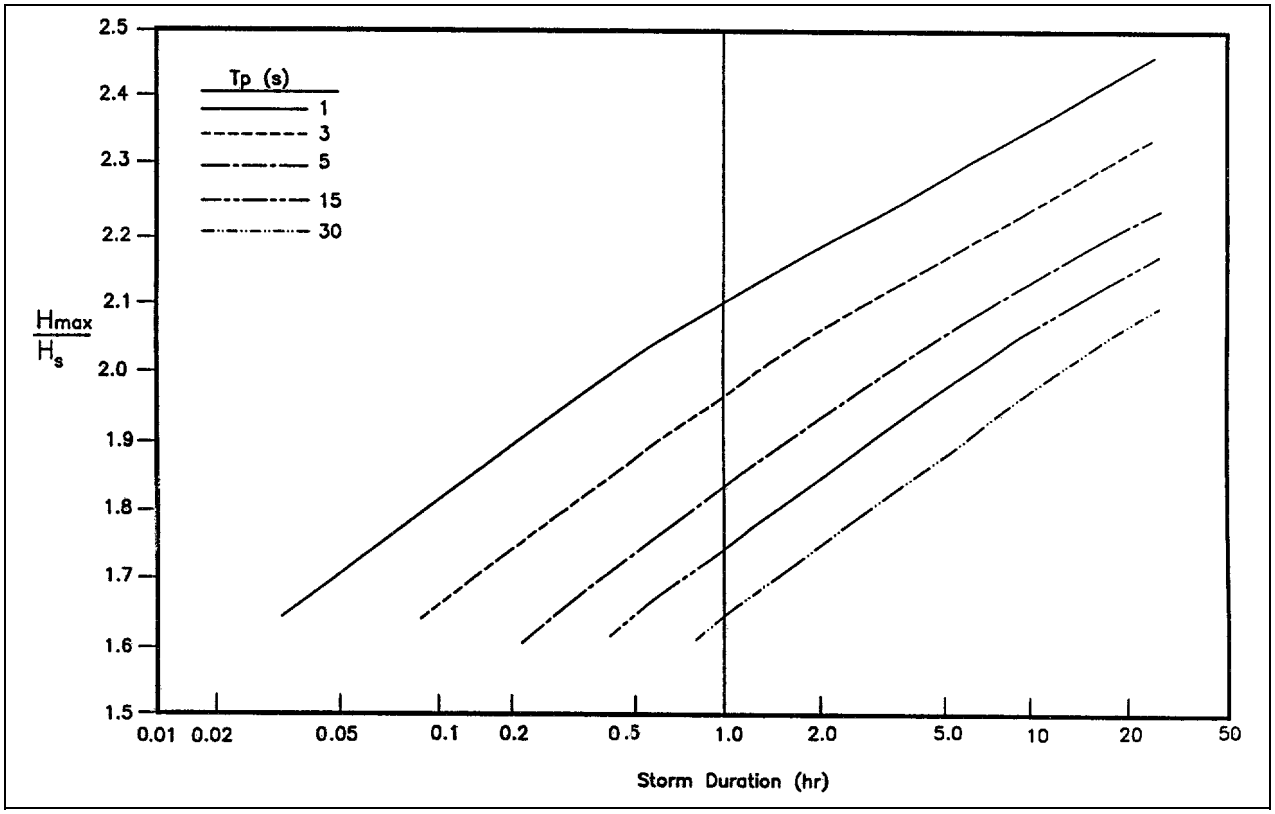

Figure 3-4. Expected maximum wave height

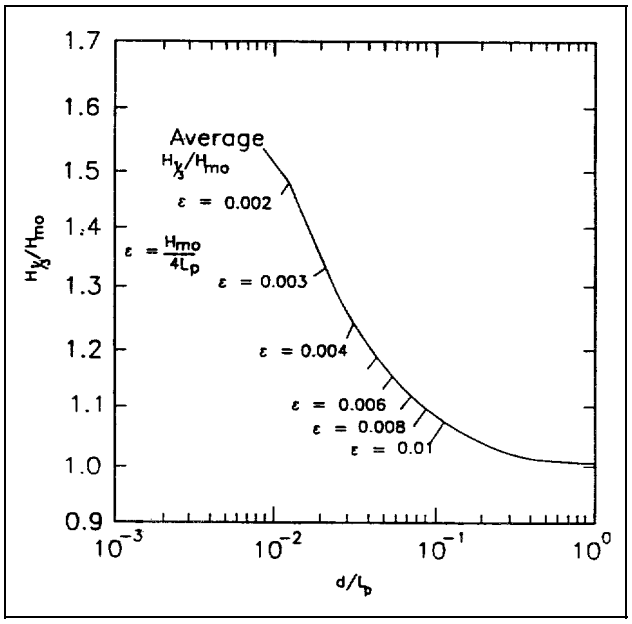

Figure 3-5. Variation in the relationship between $H_{1/3}$ and H_{mo} (after Thompson and Vincent 1985)

obtained from the significant height data and a model for the distribution of the individual wave heights. Consideration of different statistical populations may be required. The basic approaches for predicting extreme wave conditions are the extrapolation of a long-term distribution of significant wave heights, and extreme value analysis with annual maxima or with peak significant wave heights of major storms above a certain threshold. For a detailed description of these methods, the reader is directed to Chapter 5 of EM 1110-2-1414. Brief descriptions of the methods are given below.

(1) The first approach, extrapolation of a long-term distribution of significant wave heights, is relatively easy to apply. However, care must be taken concerning any statistical dependency among successive observations. A method for correcting for statistical dependency is given by Nolte (1973). The long-term distribution for wave height is usually represented by the cumulative probability distribution of the data. It is also often fit with a model distribution function. There is no strong theoretical basis for a particular model. Several models are widely used because of their success at describing

measured waves; these models are further discussed in EM 1110-2-1414.

(2) Applying extreme value analysis with annual maxima or peak significant wave heights of major storms above a certain threshold is more detailed than the first approach. In general, a probability value is assigned to each extreme data point, and the data are ordered according to wave height. These points are then plotted on an extreme value probability paper or construct paper using a wave height relationship for the abscissa and ordinate scales. A straight line is drawn through the points to represent the trend. The line can then be extrapolated to locate a design value corresponding to a chosen return period or encounter probability. The return period is the average time interval between successive events of the design wave being equaled or exceeded. The encounter probability is the probability that the design wave is equaled or exceeded during a prescribed time period. The computer program WAVDIS1 can be used to estimate the parameters of three commonly used extremal probability distributions; WAVDIS2 is an alternate version of WAVDIS1 that estimates parameters by the method of moments. The computer program FWAVOCUR is used to determine the expected frequency of extreme wave conditions over a specified period of time. These computer programs are available through the MACE program and are briefly outlined in Appendix E.

3-3. Wave Data

There are a number of sources for obtaining wave data. These include ship observations, NOAA buoys, Littoral Environment Observations (LEO), and the Wave Information Studies (WIS). A listing of publications which contain extensive summaries of meteorological and oceanographic data is given in Table 3-4. In addition to wave and water level data, the sources listed can include wind speed and direction, air and sea temperatures and other information required for wave and water level studies. Access to coastal wave and water level data is described in Table 3-5. The telephone numbers provided in Table 3-5 are for the points of contact for the programs. The points of contact for each program will instruct potential users on how to access the systems. In addition, information may be available from the Coast Guard, port and harbor authorities, and local universities. Several of these sources are summarized in Table 3-6.

a. WIS data.

(1) The Wave Information Study (WIS) was initiated by the Corps of Engineers to produce a wave climate for U.S. coastal waters. The study was divided into three main phases (Corson et al. 1982).

Phase I (Deep Ocean) are numerical hindcasts of deep water wave data from historical synoptic surface pressure charts and shipboard observations of wind velocity. Spatial grids are on the order of 2 degrees and the time increments are greater than 6 hours. The primary wave processes are air-sea and wave interactions.

Phase II (Shelf Zone) are numerical hindcasts using the same meterological information as in Phase I, but at a finer scale to better resolve the sheltering effects of the continental geometry. Phase I data serve as the boundary conditions at the seaward edge of the Phase II grid. The grid size is 0.5 degree and the time step is 3 to 6 hours. The wave processes are air-sea and wave-wave interactions.

Phase III (Nearshore Zone) is the transformation of the Phase II wave data into shallow water.

(2) Phases I, II, and III have been completed for the Atlantic and Pacific coasts. The Gulf of Mexico hindcast with a 2-degree grid (Phase I) was omitted since it is a relatively small water body compared to the Atlantic and Pacific Oceans. The Great Lakes were hindcast with a 16-km (10-mile) grid.

(3) Phase II wave estimates are provided for 71 stations along the Atlantic coast, 53 stations along the Pacific coast of California, Oregon, and Washington, and 50 stations along the Gulf coast. Hindcasts were conducted at 3-hour intervals. Tables are provided for each station which summarize the percent occurrence of wave height and period by direction. Tables are also given for the mean and largest significant wave heights by month for the 20-year hindcast.

(4) Phase III transformations from Phase II wave information are available for the Atlantic coast and Pacific coast north of Pt. Conception, California. The coastal reaches are shown in Figures 3-6 and 3-7. A Phase II hindcast was conducted for the region south of Pt. Conception to the Mexican border (Figure 3-8). Wave information on the Great Lakes is available at

Table 3-4
Summary Sources of Meteorological and Oceanographic Data

Changery, M.J. 1978 (December). "National Wind Data Index: Final Report," National Climatic Data Center, Asheville, NC 28801.

Hatch, W.L. 1983 (July). "Selective Guide to Climatic Data Sources," Key to Meteorological Records Documentation No. 4.11, National Climatic Data Center, Asheville, NC 28801.

National Oceanic and Atmospheric Administration. 1985 (May). "Index of Tide Stations: United States of America and Miscellaneous Other Stations," National Ocean Service, Tidal Datum Section, Rockville, MD 20852.

National Oceanic and Atmospheric Administration. 1985 (November). "National Ocean Service Products and Services Handbook," NOS, Sea and Lake Levels Branch, Rockville, MD 20852.

US Army Engineer Waterways Experiment Station. 1985 (October). "WES Engineering Computer Programs Library Catalog," Vicksburg, MS 39180-6199.

US Department of Commerce. 1977. "Climatic Atlas of the Outer Continental Shelf Waters and Coastal Regions of Alaska," Research Unit No. 347, National Climatic Data Center, Asheville, NC 28801.

US Department of Commerce, National Climatic Data Center. 1986 (April). "Climatic Summaries for NDBC Data Buoys," National Data Buoy Center, NSTL Station, MS 39529.

US Navy, Naval Oceanography Command. 1983 (October). "US Navy Hindcast, Spectral, Ocean Wave Model Climatic Atlas: North Atlantic Ocean," NAVAIR 50-1C-538, Naval Oceanography Command, NSTL Station, MS 39529.

Table 3-5
Sources of Coastal Wave and Water Level Data

Source	Type of Information
OL-A USAF Environmental Technical Applications Center (MAC) Federal Building Asheville, NC 28801 (704) 259-0218 (Non-Department of Defense users should contact the National Climatic Data Center at the above address.) (704) 259-0682	Global, meteorological, and oceanographic data and data products.
National Oceanographic Data Center User Service (Code OC21) 1825 Connecticut Ave., NW Washington, DC 20235 (202) 673-5549	Variety of oceanographic data.
Coastal Engineering Information and Analysis Center USAEWES 3909 Halls Ferry Rd. Vicksburg, MS 39180-6199 (601) 634-2012	Coastal Engineering Information Management (CEIMS) LEO Retrieval System, gage data from the Corps Coastal Field Data Collection Program and other sources.
Coastal Oceanography Branch USAEWES 3909 Halls Ferry Rd. Vicksburg, MS 39180-6199 (601) 634-2028	State-of-the-art computer programs for wave growth and transformation, WIS hindcast wave parameters, and two-dimensional spectra.

(Continued)

Table 3-5. (Concluded)

Source	Type of Information
Corps Computer Programs Library USAEWES IM-RS 3909 Halls Ferry Rd. Vicksburg, MS 39180-6199 (601) 634-2300	Documented computer programs for wave measurement analysis and wave growth and transformation.
Automated Coastal Engineering Group USAEWES 3909 Halls Ferry Rd. Vicksburg, MS 39180-6199 (601) 634-2017	Wave and tide analysis programs.
National Geophysical Data Center NOAA E/GC 3 325 Broadway Boulder, CO 80303 (303) 497-6388	Digital bathymetric data for United States coasts, including Alaska, Hawaii, and Puerto Rico.
California Coastal Data Information Program Scripps Institute of Oceanography Mail Code A022 University of California, San Diego LaJolla, CA 92093 (619) 534-3033	United States west coast gage network and gage at CERC's FRF in North Carolina.
Field Coastal Data Network Coastal & Oceanographic Engineering Department 336 Weil Hall University of Florida Gainesville, FL 32611 (904) 392-1051	Coastal Florida wave gage network.
Navy/NOAA Oceanographic Data Distribution system operated by: Science Applications International Corporation 205 Montecito Avenue Monterey, CA 93940 (408) 375-3063	Global forecast wave and weather data.
NOAA National Ocean Service Tidal Datums and Information Section 6001 Executive Blvd. Rockville, MD 20852 (301) 443-8467	Tidal table, tidal current tables, and digital data for selected locations.
Alaska Coastal Data Collection Program Plan Formulation Section US Army Engineer District, Alaska Pouch 898 Anchorage, AK 99506-0898 (907) 753-2620	Wind and wave data for coastal Alaska.

Table 3-6
Additional Sources of Meteorological and Oceanographic Data

The Sea State Engineering Analysis System (SEAS) enables Corps users to access WIS data and form a variety of summaries. SEAS is a user-friendly system which consists of a data base of hindcast wave parameters, a retrieval system, and a library of statistical routines to produce desired summaries.

An interactive system developed at Scripps Institute of Oceanography (SIO) is available for accessing parameters from the SIO-based network of wave gages. The network includes primarily west coast gages, many of which are supported by the Corps' Coastal Field Data Collection Program.

A system similar to SIO's interactive system is operated by the University of Florida for wave gages along the Florida coast.

Global forecast wave and weather information is available through the Navy/NOAA Oceanographic Data Distribution System (NODDS). The forecast wave data are calculated using the Navy's Global Spectral Ocean Wave Model. NODDS is operated by Science Applications International Corporation under contract to the Jet Propulsion Laboratory.

CEIMS is a computerized system being developed by CERC. It will provide indexes to a wide variety of coastal data. It will also provide direct access to selected data sets and processing programs.

An interactive environmental data reference service is described in Blumenthal and O'Quinn (1981).

stations 16 km (10 miles) apart as shown in Figure 3-9. Gulf Coast stations are shown in Figure 3-10. The Phase III results bring the hindcast waves into the nearshore. If these data are available at a design site, they should be included in the design wave selection. WIS reports are listed in Table 3-7.

b. LEO data.

(1) The Corps of Engineers program for collection of wave observations from shore is the Littoral Environment Observation (LEO) program. The LEO program was established to provide data on coastal phenomena at low cost. Volunteer observers obtain daily estimates which include the breaker height, wave period, direction of wave approach, wind speed, wind direction, current speed, and current direction. Wave height and direction are visual estimates. Other parameters are estimated with simple equipment. The skill of individual observers significantly influences the validity of the observations from shore.

(2) The locations of active LEO sites are shown in Figure 3-11. Generally, LEO data are tabulated annually as scatter diagrams of the percent occurrence of waves in different wave height-wave period categories. To be statistically descriptive of a site, observations must be recorded for at least 20 days of each month for a period of at least 3 years. Additional information on the LEO program is given in Schneider (1981), and Sherlock and Szuwalski (1987).

c. NOAA buoy data. Since 1972 the National Oceanic and Atmospheric Administration (NOAA) has maintained a number of oceanographic buoys throughout United States coastal waters. Table 3-8 gives locations of the NOAA buoys and years of information through 1988. Further updates or actual buoy data can be obtained from the National Oceanographic Data Center. Available information includes wind direction and speed, sea level pressure, air temperature, sea surface temperature, significant wave height, dominant wave period, and peak gust data (US Department of Commerce 1990).

d. Ship observations.

(1) Wave observations have been collected by observers aboard ships in passage for many areas of the world over many years. The observations include average wave height, period, and direction of the sea waves (locally generated) and the swell waves (generated elsewhere and propagated to the area). In modern observations, the sea direction is assumed to coincide with the wind direction.

(2) The reliability of shipboard observations must be considered. Individual observations are highly variable, and the accuracy of reported wave heights is lower for high energy conditions. There are a limited number of high energy observations because ships tend to avoid storms, and measurements made under these conditions are less reliable. A cumulative distribution of shipboard

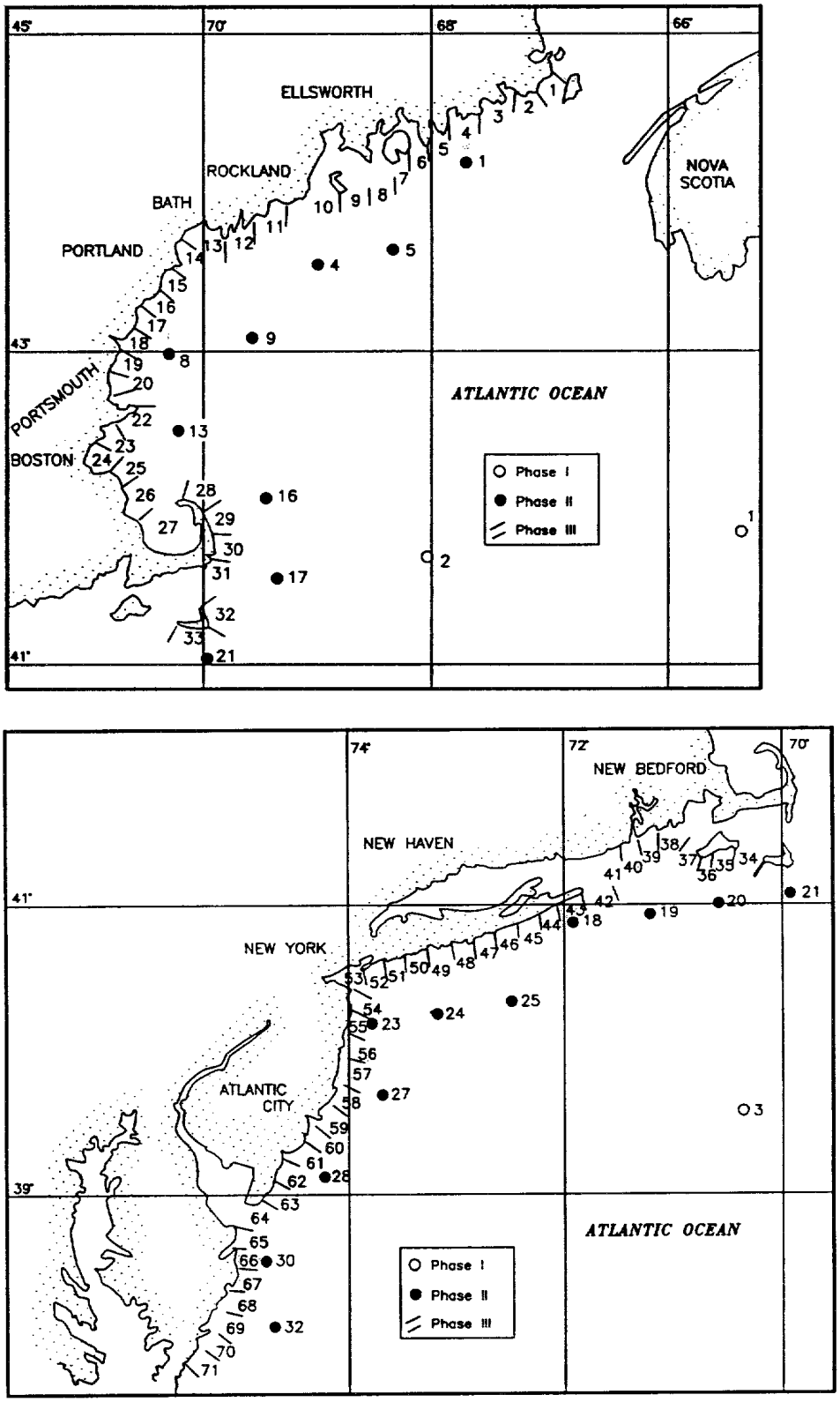

Figure 3-6. Atlantic coast locations of WIS Phase II and III information (Sheet 1 of 3)

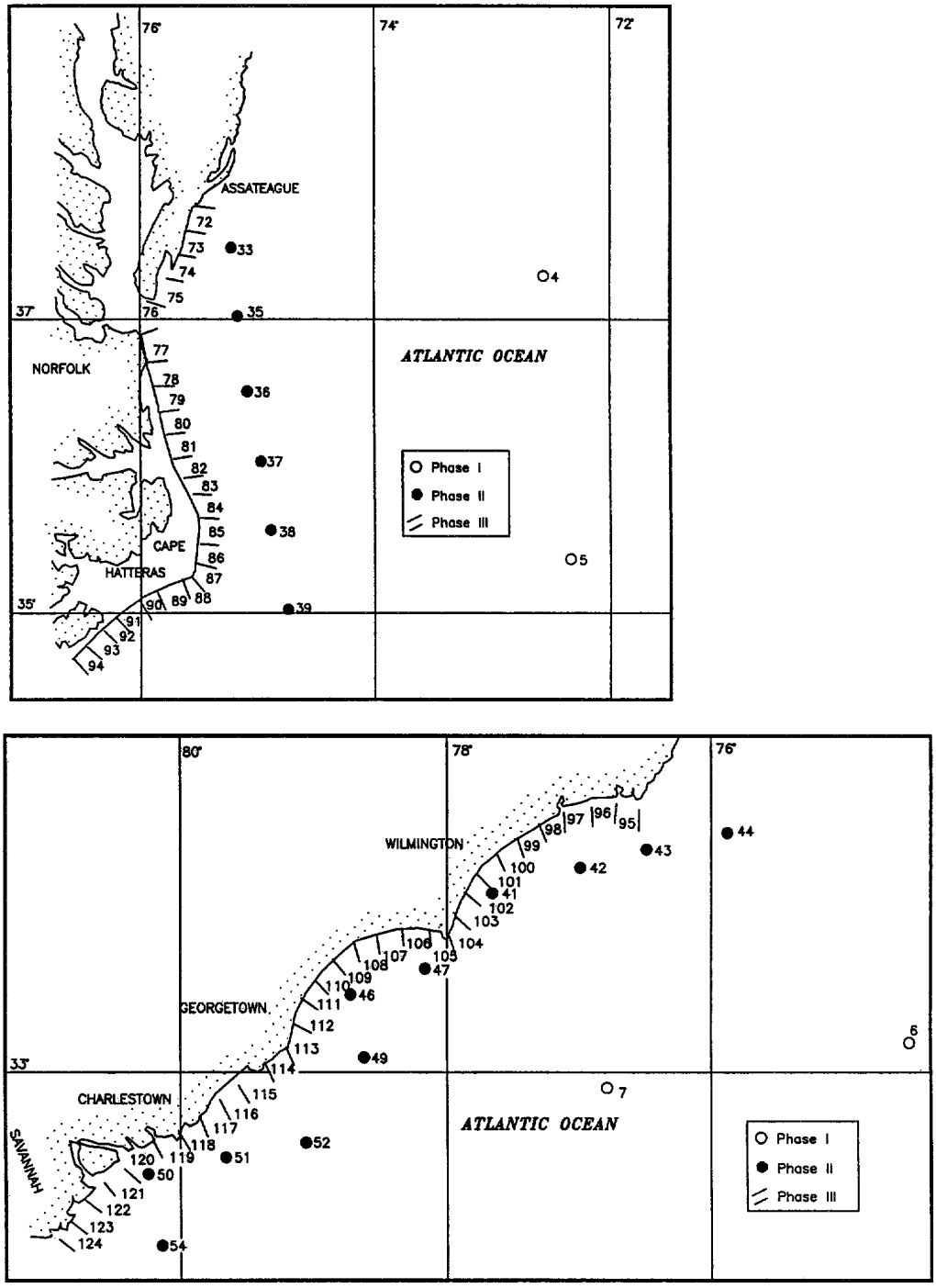

Figure 3-6. (Sheet 2 of 3)

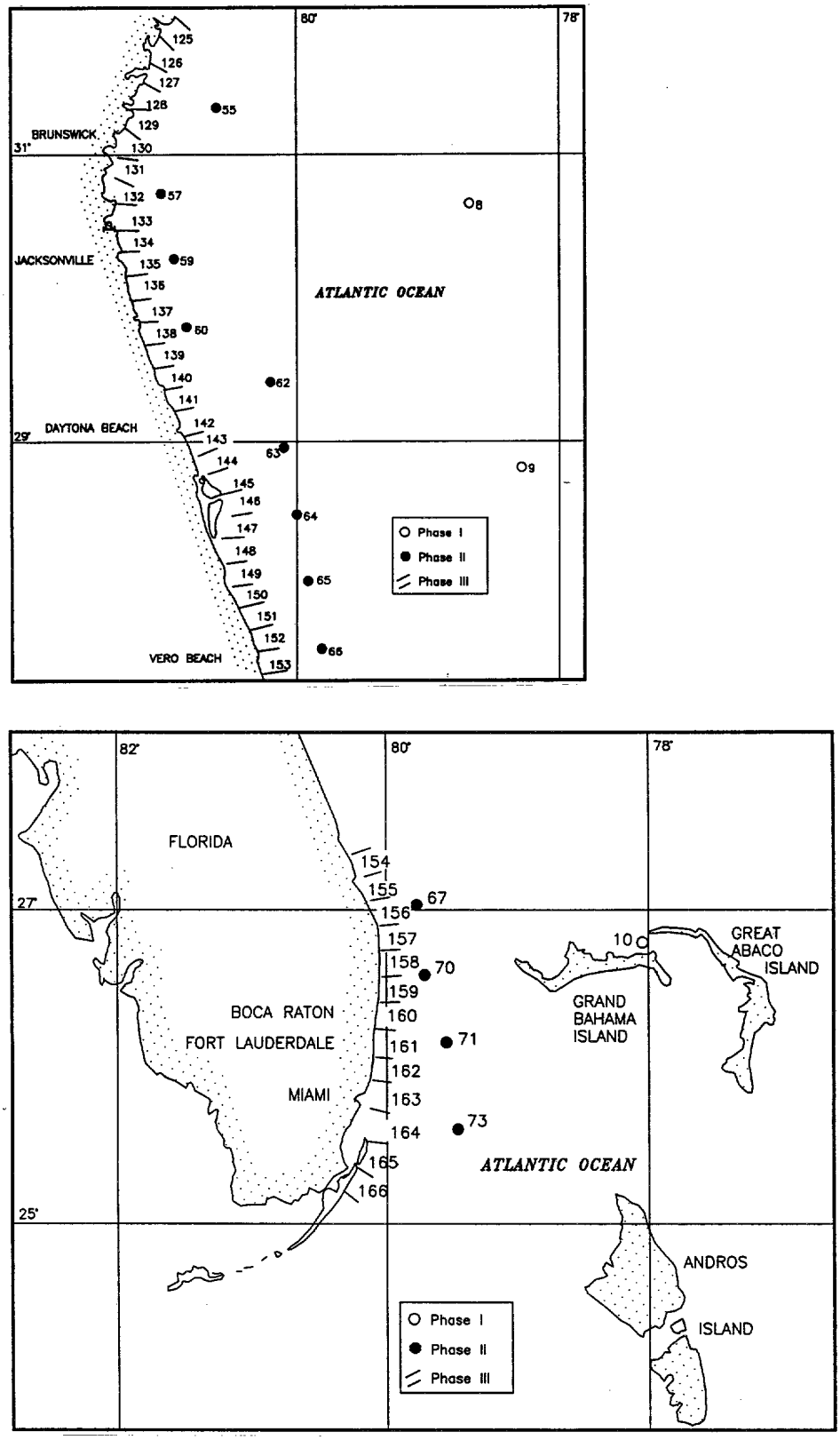

Figure 3-6. (Sheet 3 of 3)

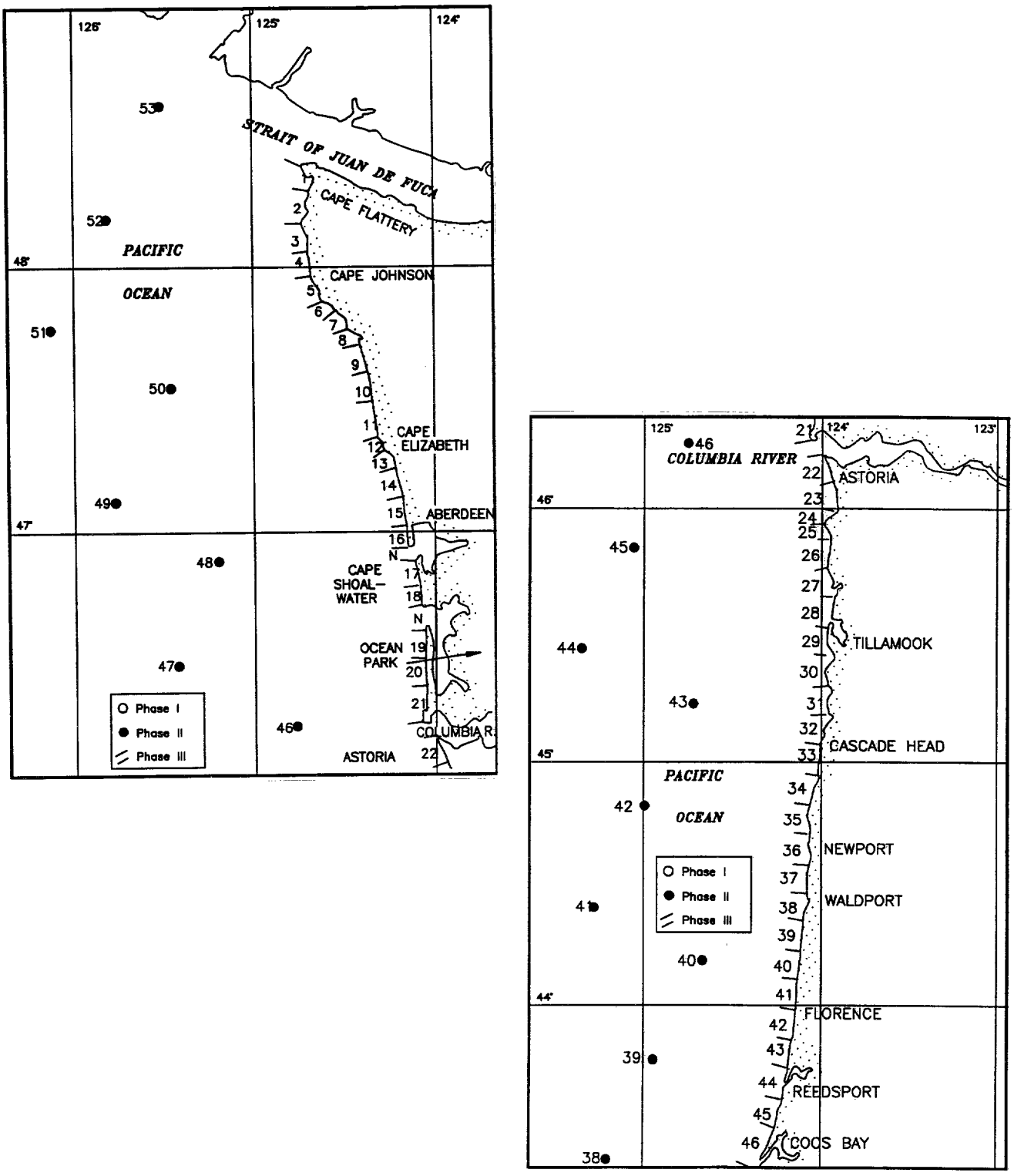

Figure 3-7. Pacific coast locations of WIS Phase II and III information (Sheet 1 of 3)

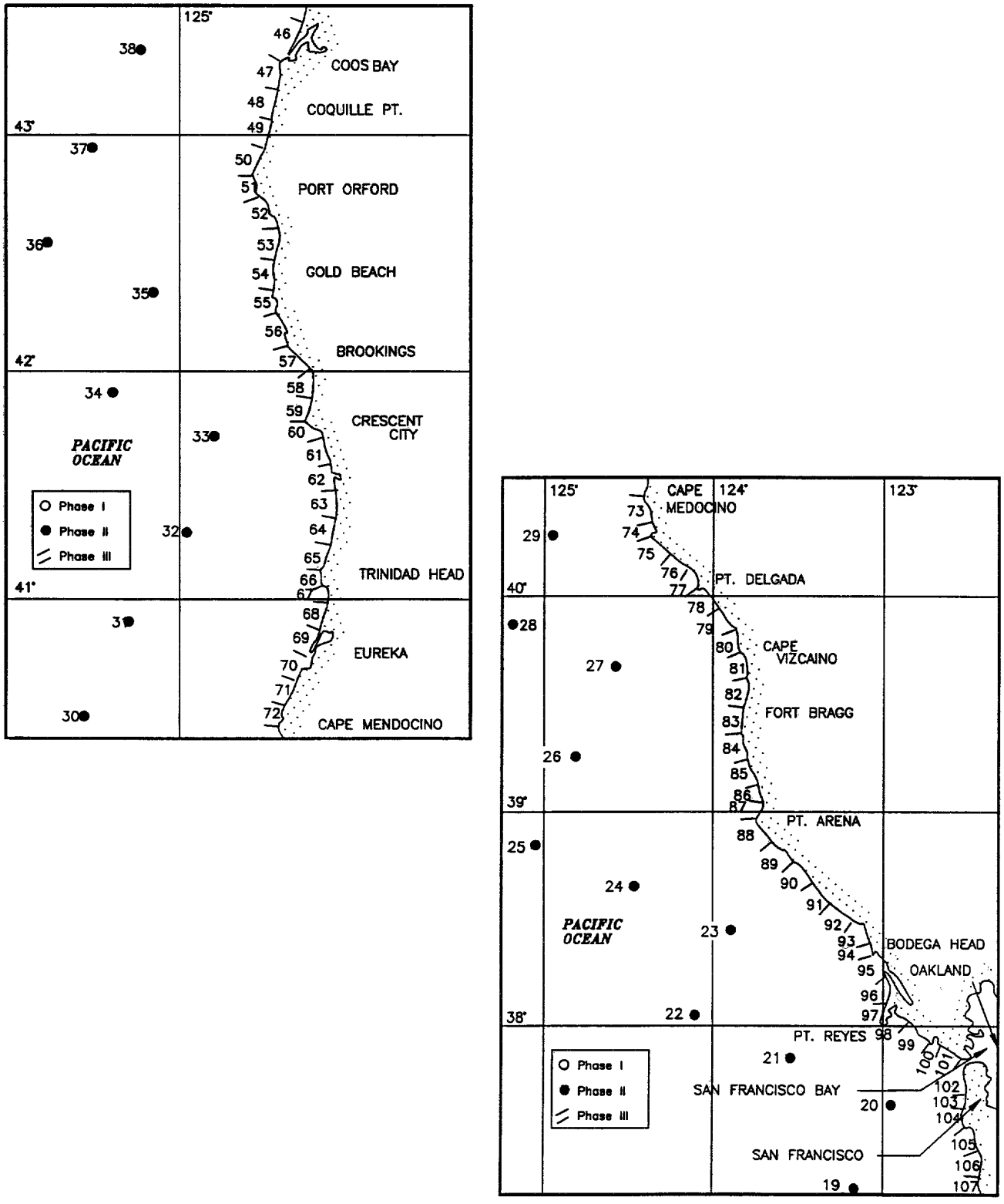

Figure 3-7. (Sheet 2 of 3)

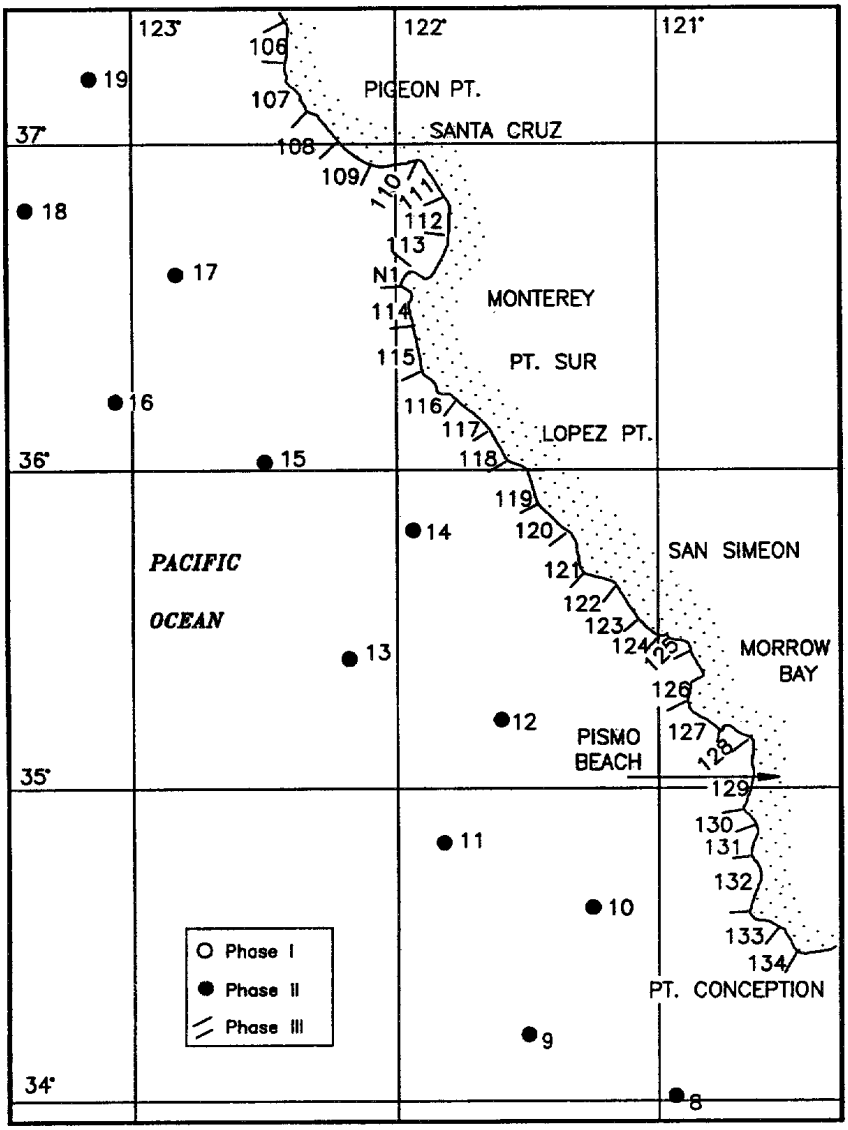

Figure 3-7. (Sheet 3 of 3)

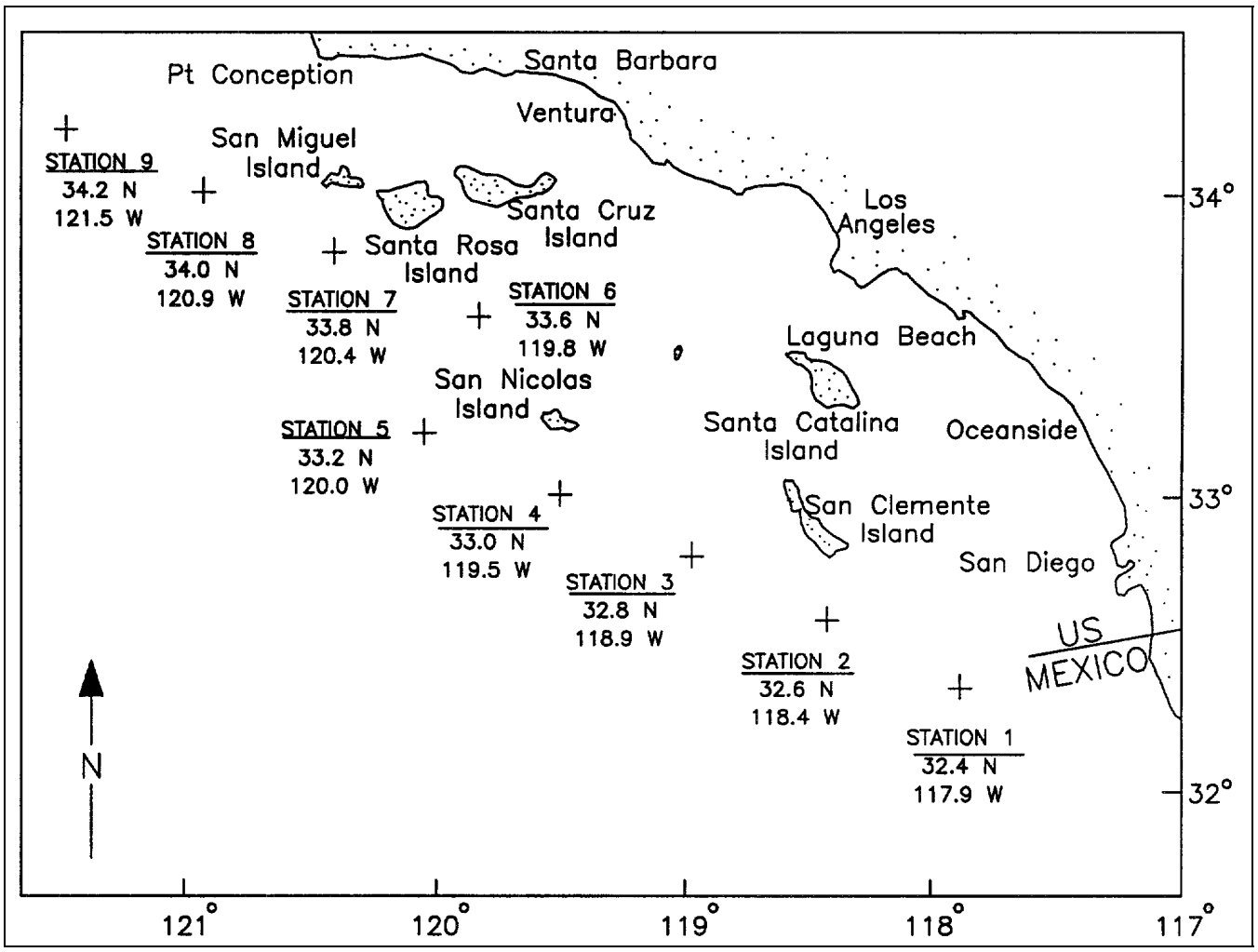

Figure 3-8. WIS Phase II locations for Southern California Bight

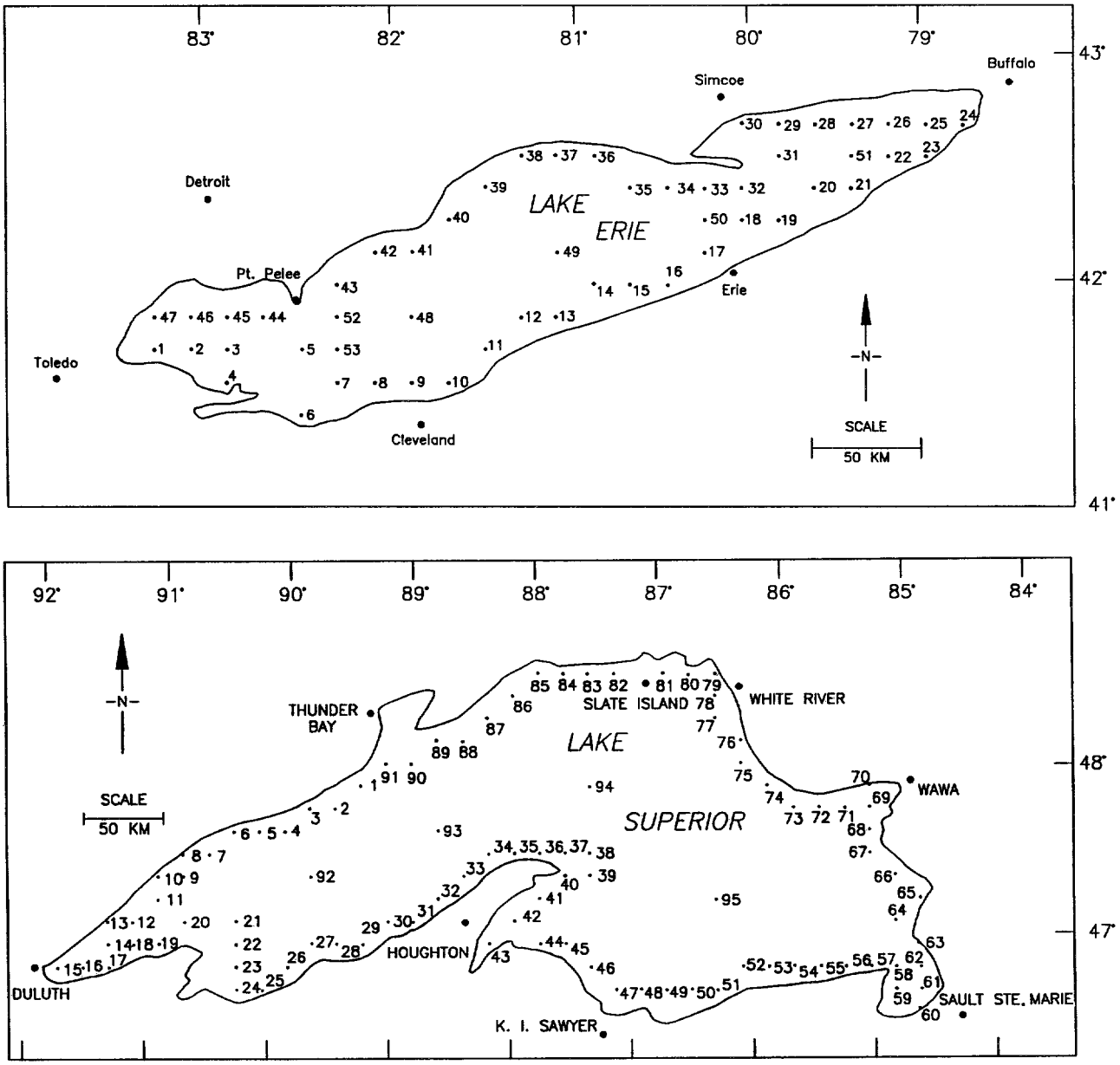

Figure 3-9. Great Lakes hindcast stations (Sheet 1 of 3)

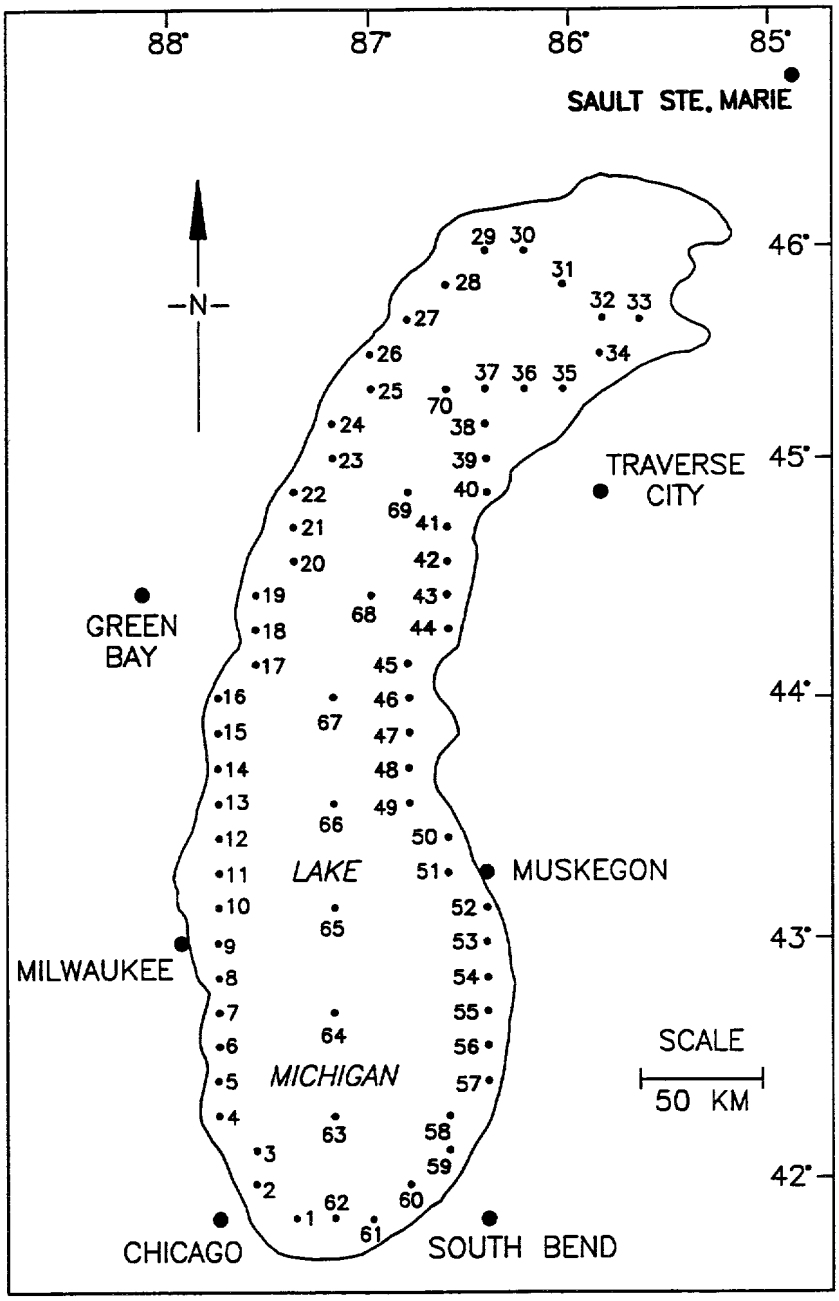

Figure 3-9. (Sheet 2 of 3)

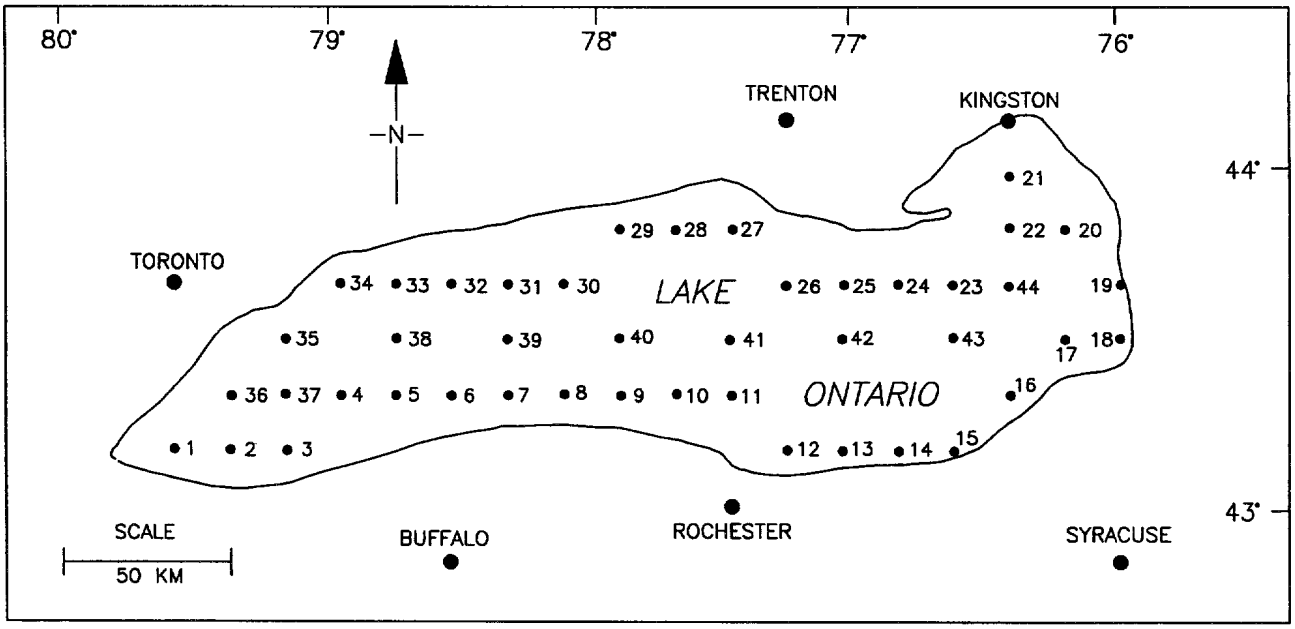

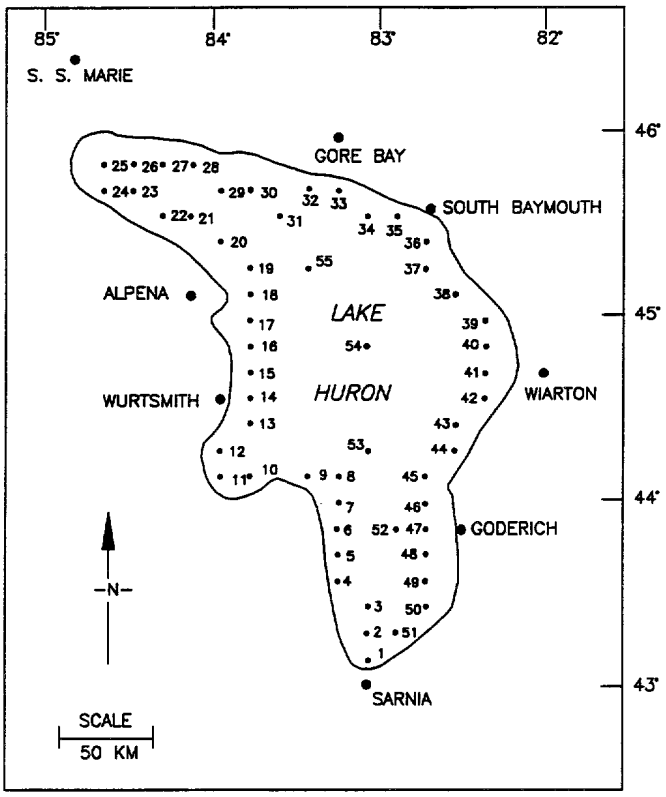

Figure 3-9. (Sheet 3 of 3)

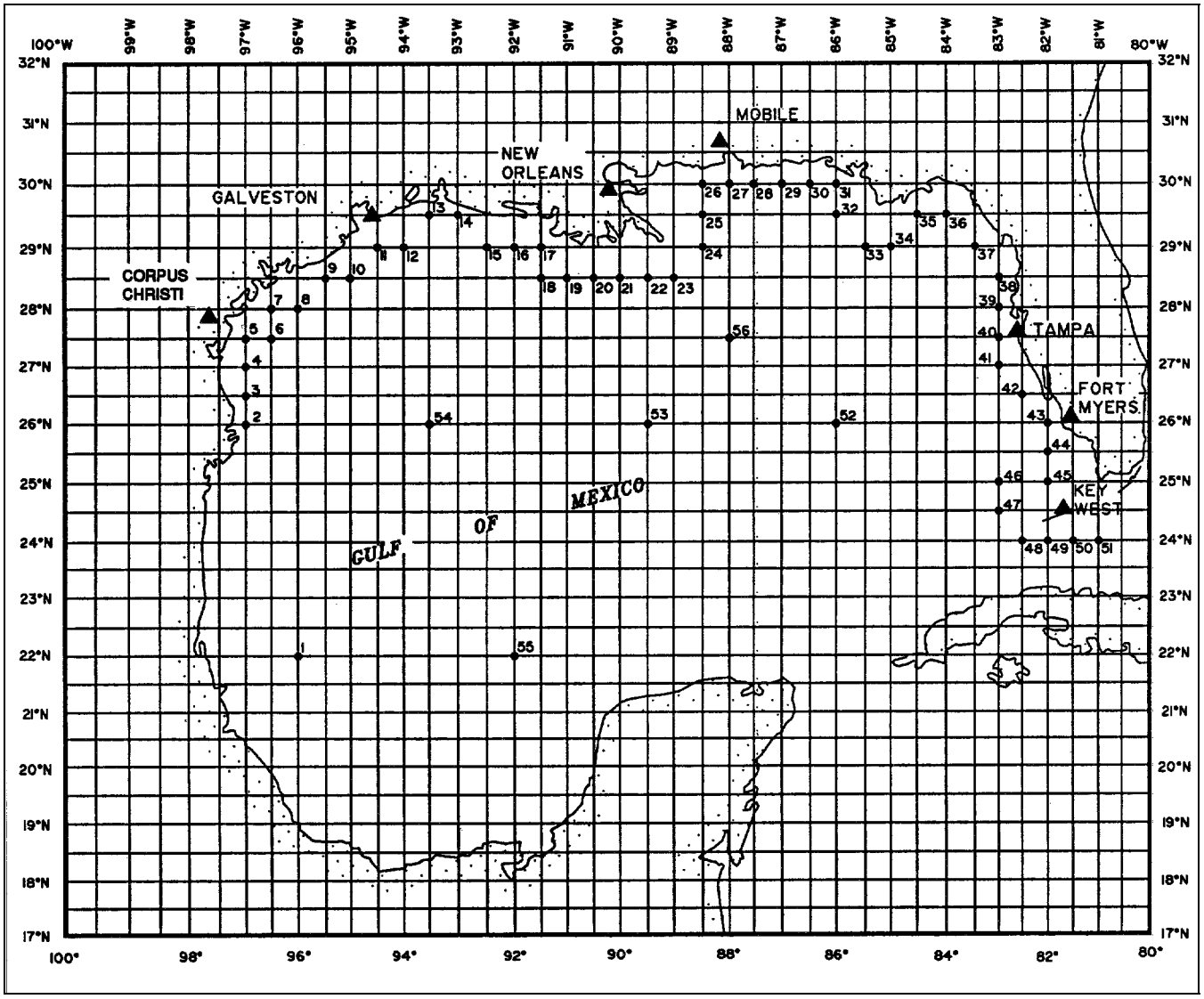

Figure 3-10. Gulf coast locations of WIS phase II information

Table 3-7
Wave Information Studies (WIS) Reports

Bibliographic Information

Atlantic and Pacific Coasts Reports

Corson, W. D., Resio, D. T., and Vincent, C. L. 1980 (July). "Wave Information Study of U.S. Coastlines; Surface Pressure Field Reconstruction for Wave Hindcasting Purposes," TR HL-80-11, Report 1.

Corson, W. D., Resio, D. T., Brooks, R. M., Ebersole, B. A., Jensen, R. E., Ragsdale, D. S., and Tracy, B. A. 1981 (January). "Atlantic Coast Hindcast, Deepwater Significant Wave Information," WIS Report 2.

Corson, W. D., and Resio, D. T. 1981 (May). "Comparisons of Hindcast and Measured Deepwater Significant Wave Heights," WIS Report 3.

Resio, D. T., Vincent, C. L., and Corson, W. D. 1982 (May). "Objective Specification of Atlantic Ocean Windfields from Historical Data," WIS Report 4.

Resio, D. T. 1982 (March). "The Estimation of Wind-Wave Generation in a Discrete Spectral Model," WIS Report 5.

Corson, W. D., Resio, D. T., Brooks, R. M., Ebersole, B. A., Jensen, R. E., Ragsdale, D. S., and Tracy, B. A. 1982 (March). "Atlantic Coast Hindcast Phase II, Significant Wave Information," WIS Report 6.

Ebersole, B. A. 1982 (April). "Atlantic Coast Water-Level Climate," WIS Report 7.

Jensen, R. E. 1983 (September). "Methodology for the Calculation of a Shallow Water Wave Climate," WIS Report 8.

Jensen, R. E. 1983 (January). "Atlantic Coast Hindcast, Shallow-Water Significant Wave Information," WIS Report 9.

Ragsdale, D. S. 1983 (August). "Sea-State Engineering Analysis System: Users Manual," WIS Report 10.

Tracy, B. A. 1982 (May). "Theory and Calculation of the Nonlinear Energy Transfer Between Sea Waves in Deep Water," WIS Report 11.

Resio, D. T., and Tracy, B. A. 1983 (January). "A Numerical Model for Wind-Wave Prediction in Deepwater," WIS Report 12.

Brooks, R. M., and Corson, W. D. 1984 (September). "Summary of Archived Atlantic Coast Wave Information Study, Pressure, Wind, Wave, and Water Level Data," WIS Report 13.

Corson, W. D., Abel, C. E., Brooks, R. M., Farrar, P. D., Groves, B. J., Jensen, R. E., Payne, J. B., Ragsdale, D. S., and Tracy, B. A. 1986 (March). "Pacific Coast Hindcast, Deepwater Wave Information," WIS Report 14.

Corson, W. D., and Tracy, B. A. 1985 (May). "Atlantic Coast Hindcast, Phase II Wave Information: Additional Extremal Estimates," WIS Report 15.

Corson, W. D., Abel, C. E., Brooks, R. M., Farrar, P. D., Groves, B. J., Payne, J. B., McAneny, D. S., and Tracy, B. A. 1987 (May). "Pacific Coast Hindcast Phase II Wave Information," WIS Report 16.

Jensen, R. E., Hubertz, J. M., and Payne, J. B. 1989 (Mar). "Pacific Coast Hindcast, Phase III North Wave Information," WIS Report 17.

Hubertz, J. M., and Brooks, R. M. 1989 (Mar). "Gulf of Mexico Hindcast Wave Information," WIS Report 18.

Abel, C. E., Tracy, B. A., Vincent, C. L., and Jensen, R. E. 1989 (Apr). "Hurricane Hindcast Methodology and Wave Statistics for Atlantic and Gulf Hurricanes from 1956-1975," WIS Report 19.

Jensen, R. E., Hubertz, J. M., Thompson, E. F., Reinhard, R. D., Groves, B., Brown, W. A., Payne, J. B., Brooks, R. M., and McAneny, D. S. (In preparation). "Southern California Hindcast Wave Information," WIS Report 20.

Tracy, B. A., and Hubertz, J. M. (In preparation). "Hindcast Hurricane Swell for the Coast of Southern California," WIS Report 21.

(Continued)

Table 3-7. (Concluded)

Bibliographic Information
Great Lakes Reports
Resio, D. T., and Vincent, C. L. 1976 (January). "Design Wave Information for the Great Lakes; Report 1: Lake Erie," TR H-76-1.
Resio, D. T., and Vincent, C. L. 1976 (March). "Design Wave Information for the Great Lakes; Report 2: Lake Ontario," TR H-76-1.
Resio, D. T., and Vincent, C. L. 1976 (June). "Estimation of Winds Over Great Lakes," MP H-76-12.
Resio, D. T., and Vincent, C. L. 1976 (November). "Design Wave Information for the Great Lakes; Report 3: Lake Michigan," TR H-76-1.
Resio, D. T., and Vincent, C. L. 1977 (March). "Seasonal Variations in Great Lakes Design Wave Heights: Lake Erie," MP H-76-21.
Resio, D. T., and Vincent, C. L. 1977 (August). "A Numerical Hindcast Model for Wave Spectra on Water Bodies with Irregular Shoreline Geometry," Report 1, MP H-77-9.
Resio, D. T., and Vincent, C. L. 1977 (September). "Design Wave Information for the Great Lakes; Report 4: Lake Huron," TR H-76-1.
Resio, D. T., and Vincent, C. L. 1978 (June). "Design Wave Information for the Great Lakes; Report 5: Lake Superior," TR H-76-1.
Resio, D. T., and Vincent, C. L. 1978 (December). "A Numerical Hindcast Model for Wave Spectra on Water Bodies with Irregular Shoreline Geometry," Report 2, MP H-77-9.

Note:
All reports listed above were published by and are available from the US Army Engineer Waterways Experiment Station, Coastal Engineering Research Center, 3909 Halls Ferry Road, Vicksburg, MS 39180-6199

observed wave heights should be considered reliable up to about the one percent level of occurrence or the point at which 20 observations are represented, whichever criterion is more restrictive.

(3) Wave period is difficult to estimate aboard a moving ship, and only the overall mean period should be used. Wave directions are also somewhat difficult to estimate and should be assumed to have a resolution of 45 degrees or coarser.

3-4. Wave Hindcasting

WIS results may not be available for a specific time period of interest or wave measurements may not be available at the design site of sufficient quality or quantity to allow direct determination of the design wave. However, reasonable weather data are often available so this information may be used to hindcast waves. Waves that are generated by a storm are a function of the wind speed U, the duration of the storm t, and how large an area the storm covers, or fetch length F. Table 3-9 is a qualitative description of the sea state as a function of the wind speed and typical wave conditions. These descriptions are for a fully arisen sea state that requires a minimum duration to develop. These values should not be used for design, but rather to appreciate various sea states.

a. Predictive methods.

(1) There are a variety of techniques and computer models available for predicting sea states as a function of storm conditions. The more complex models can provide estimates of wave height, wave period, and direction as well as the frequency distribution of energy. These types of models were used to generate the WIS results. However, there are cases where neither the time available nor the cost justifies using a complex numerical method. In these situations, simplified methods may be appropriate. The wave hindcasting method outlined in this manual follows the technique described in more detail in the Shore Protection Manual (1984). In this simplified technique, the significant wave height and period are estimated from the wind stress, storm duration, and fetch length.

(2) Unfortunately, there are a variety of locations (i.e., over land, over water, or different elevations) and techniques for presenting wind measurements. If measured wind speeds are provided, care must be taken to convert to the appropriate wind speeds for wave hindcasting. These corrections are given in the Shore Protection Manual (1984) in Chapter 3, Section IV. A

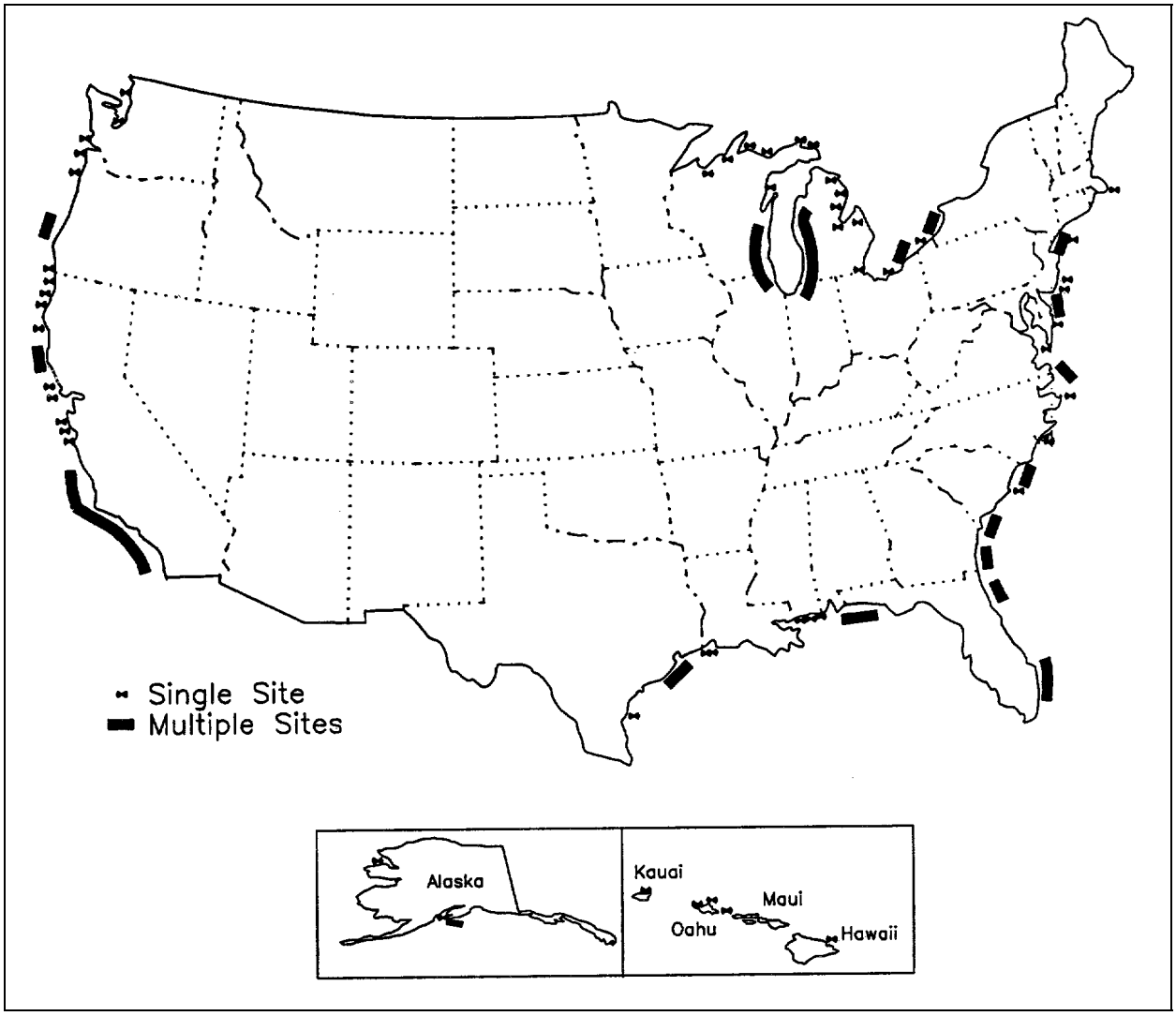

Figure 3-11. Leo sites

Table 3-8
NOAA Buoy Locations and Years (US Department of Commerce 1990)

Station No.	Latitude, °N	Longitude, °W	Years
	Great Lakes		
45006	47.3	90.0	81-88
45001	48.0	87.6	79-88
45004	47.2	86.5	80-88
45002	45.3	86.3	79-88
45007	42.7	87.1	81-88
45003	42.7	87.1	80-88
45008	44.3	82.4	81-88
45005	41.7	82.5	80-88
	Atlantic		
44007	43.5	70.1	82-88
44005	42.7	68.3	78-88
44013	42.4	70.8	84-88
44003	40.8	68.5	77-84
44011	41.1	66.6	84-88
44002	40.1	73.0	75-80
44008	40.5	69.4	82-88
44012	38.8	74.6	84-88
44004	38.5	70.7	77-88
44001	38.7	73.6	75-79
44009	38.5	74.6	84-88
CHLV2	36.9	75.7	84-88
41001	34.9	72.9	72-88
41002	32.3	75.3	74-88
41004	32.6	78.7	78-82
41005	31.7	79.7	79-82
41003	30.3	80.4	77-82
41006	29.3	77.3	82-88
	Gulf of Mexico		
42009	29.3	87.5	80-86
42007	30.1	88.9	81-88
	Gulf of Mexico (Cont'd)		
42001	29.6	93.5	81-84
42008	28.7	85.3	80-84
42002	26.0	93.5	76-88
42001	25.9	89.7	75-88
42003	26.0	85.9	76-88
	Pacific		
46016	63.3	170.3	81-84
46017	60.3	172.3	81-84
46001	56.3	148.2	72-88
46003	51.9	155.7	76-88
46004	51.0	136.0	76-88
46005	46.1	131.0	76-88
46010	46.2	124.2	79-88
46029	46.2	124.2	84-87
46006	40.7	137.7	77-88
46002	42.5	130.3	75-88
46027	41.8	124.4	83-88
46022	40.8	124.5	82-88
46014	39.2	124.0	81-88
46013	38.2	123.3	81-88
46026	37.8	122.7	82-88
46012	37.4	122.7	80-88
46028	35.8	121.7	83-88
46011	34.9	120.9	80-88
46023	34.3	120.7	82-88
46024	33.8	119.5	82-84
46025	33.6	119.0	82-88
51001	23.4	162.3	81-88
51003	19.2	160.8	84-88
51002	17.2	157.8	84-88
51004	17.5	152.6	84-88

common way to estimate the wind speed is from surface synoptic charts. These are available from the US Weather Service. An example synoptic chart is given in Figure 3-12. The pressure isobars are typically contoured at either 3 or 4 millibar (mb) intervals. This particular chart has a contour interval of 4 mb. Since the pressure is usually around 1000 mb, it is only necessary to record the last two digits of the pressure on the isobars. The pressure gradients indicated by the isobars are primarily due to density differences in the air. This pressure gradient is nearly in equilibrium with the Coriolis force produced by the rotation of the earth. The geostrophic wind is defined by assuming that an equilibrium or exact balance exists. The geostrophic wind blows approximately parallel to the isobars with low pressure to the left when looking in the direction of the wind in the northern hemisphere. In the southern hemisphere, the low pressure is on the right. The geostrophic wind is usually the best simple estimate of the wind speed. Figure 3-13 may be used to determine the geostrophic wind speed. The geostrophic wind speed depends on the latitude, the average pressure gradient across the fetch, and the isobar spacing on the synoptic chart.

(3) Once the geostrophic wind speed is known, several correction factors should be applied. The first of these, R_T, accounts for the air-sea temperature difference. This correction is given in Figure 3-14. If no temperature data are available, then use $R_T = 0.9$ for $T_a > T_s$, $R_T = 1.0$ for $T_a = T_s$, and $R_T = 1.1$ for $T_a < T_s$. The wave prediction curves are based on the wind speed measured at a 10-meter elevation. A correction must be applied to the geostrophic wind speed U_g to correct it

Table 3-9
Qualitative Sea State Descriptions (Meyers, Holm, and McAllister 1969)

Sea State	Description	Beaufort Wind Force	Description	U(kts)	H_s(ft)	T_p(s)
0	Sea like a mirror.	0	Calm	0	0	
1	Ripples with the appearance of scales are formed, but without foam crests.	1	Light airs	2.0	0.08	0.7
	Small wavelets, still short but more pronounced; crests have a glassy appearance, but do not break.	2	Light breeze	5.0	0.29	2.0
	Large wavelets, crests being to break. Foam of glassy appearance. Perhaps scattered white horses.	3	Gentle breeze	8.5	1.0	3.4
2				10.0	1.4	4.0
				12.0	2.2	4.8
	Small waves, becoming larger; fairly frequent white horses.	4	Moderate breeze	13.5	2.9	5.4
3				14.0	3.3	5.6
		5		16.0	4.6	6.5
	Moderate waves, taking a more pronounced long form; many		Fresh breeze	18.0	6.1	7.2
4	white horses are formed (chance of some spray).			19.0	6.9	7.7
				20.0	8.0	8.1
5	Large waves begin to form; the white foam crests are	6	Strong breeze	24.0	12.0	9.7
	more extensive everywhere (probably some spray).			24.5	13.0	9.9
6				26.0	15.0	10.5
	Sea heaps up and white foam from breaking waves begins	7	Moderate gale	28.0	18.0	11.3
	to be blown in streaks along the direction of the wind			30.0	22.0	12.1
	(spindrift begins to be seen).			30.5	23.0	12.4
				32.0	26.0	12.9
7	Moderately high waves of greater length; edges of crests	8	Fresh gale	34.0	30.0	13.6
	break into spindrift. The foam is blown in well-marked			36.0	35.0	10.3
	streaks along the direction of the wind. Spray affects			37.0	37.0	14.9
	visibility.			38.0	40.0	15.4
				40.0	45.0	16.1
8	High waves. Dense streaks of foam along the directions of	9	Strong gale	42.0	50.0	17.0
	the wind. Sea begins to roll. Visibility affected.			44.0	58.0	17.7
				46.0	64.0	18.6
		10	Whole gale	48.0	71.0	19.4
	Very high waves with long overhanging crests. The resulting foam is in great patches and is blown in dense white streaks along the direction of the wind. On the whole, the surface of the sea takes a white appearance. The rolling of the sea becomes heavy and shocklike. Visibility is affected.			50.0	78.0	20.2
				51.5	83.0	20.8
				52.0	87.0	21.0
				54.0	95.0	21.8
	Exceptional high waves (small and medium-sized ships might for a long time be lost to view behind the waves).	11	Storm	56.0	103.0	22.6
9	The sea is completely covered with long white patches of foam lying along the direction of the wind. Everywhere the edges of the wave crests are blown in froth. Visibility affected.			59.5	116.0	24.0
	Air filled with foam and spray. Sea completely white with driving spray; visibility very seriously affected.	12	Hurricane	>64.0	>128.0	(26)

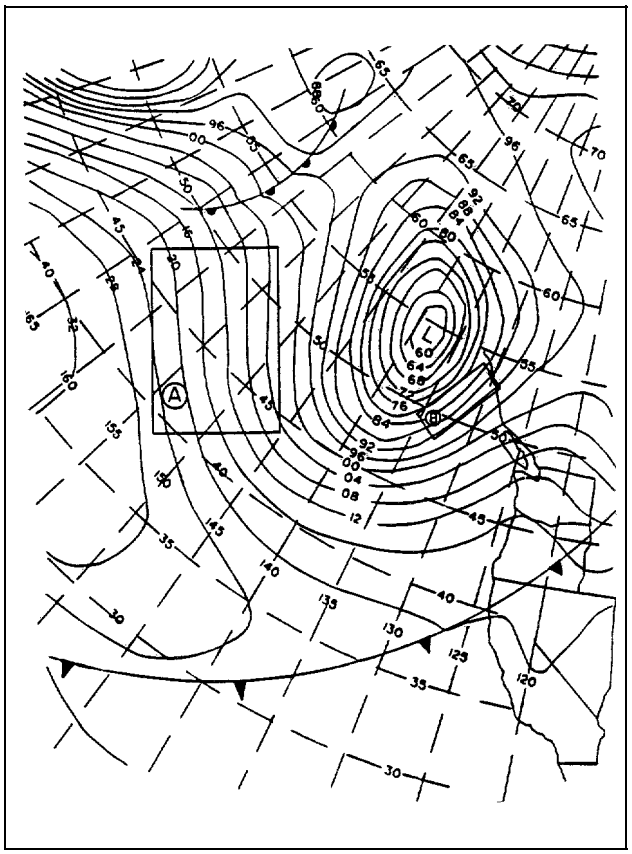

Figure 3-12. Simplified surface synoptic chart (pressure contours in millibars)

to the 10-meter wind speed U. This correction factor R_G is given in Figure 3-15. The temperature corrected 10-meter wind speed is given by

$$U = R_T \, R_G \, U_g \tag{3-5}$$

Wave growth formula diagrams are expressed in terms of a wind stress factor U_A. Wind speed is converted to a wind stress factor by

$$U_A = 0.71 \, U^{1.23} \quad (U \text{ in m/sec}) \tag{3-6}$$

(4) The fetch is the region over which the wind speed and direction are relatively constant. Results are best when variation of direction of the wind speed (assumed parallel to the isobars) does not exceed ±15 degrees. Direction deviations of 30 degrees should not be exceeded. Variations in the wind speed should not exceed ±2.5 meters/second from the mean. Since the wind speed is related to the isobar spacing, this implies that the spacing should be nearly constant across the fetch. Using these rules, several fetches have been identified on the synoptic chart in Figure 3-12. Frequently, the discontinuity at a weather front will also limit a fetch. The fetch length is simply determined by measuring the length of the fetch and noting that 5 degrees of latitude = 300 nautical miles (nmi) = 555 kilometers.

(5) Estimates of the duration of the wind are also needed for wave prediction. Complete synoptic weather charts are prepared at only 6-hour intervals. Thus, interpolation to determine the duration may be necessary. Linear interpolation is adequate in most cases.

(6) With the estimates of the wind stress factor, wind duration, and fetch length available, the deep water significant wave height and peak spectral period may be determined from Figure 3-16, or with the Automated Coastal Engineering System (ACES) program "Windspeed Adjustment and Wave Growth" (see Appendix E). For a given wind speed, the wave height can either be limited by the fetch length or the duration of the storm.

********** EXAMPLE 3-1 **********

GIVEN: The wind stress factor is 20 m/sec (66 ft/sec), the fetch length is 90 km (49 nmi), and the storm duration is 5 hours.

FIND: Determine the significant wave height and peak spectral period.

SOLUTION: From Figure 3-16, two possible wave conditions can be estimated.

1) U_A = 20 m/sec (66 ft/sec) and F = 90 km (49 nmi) yield

H_s = 3.0 m (9.8 ft) and T_P = 7.6 sec

2) U_A = 20 m/sec (66 ft/sec) and t = 5 hours yield

H_s = 2.5 m (8.2 ft) and T_P = 6.6 sec

The smaller of these two should be selected. Since the duration yields the smaller wave, this wave is termed duration limited. If the duration had been greater than 6.5 hours, then the wave would have been fetch limited.

********** END EXAMPLE 3-1 **********

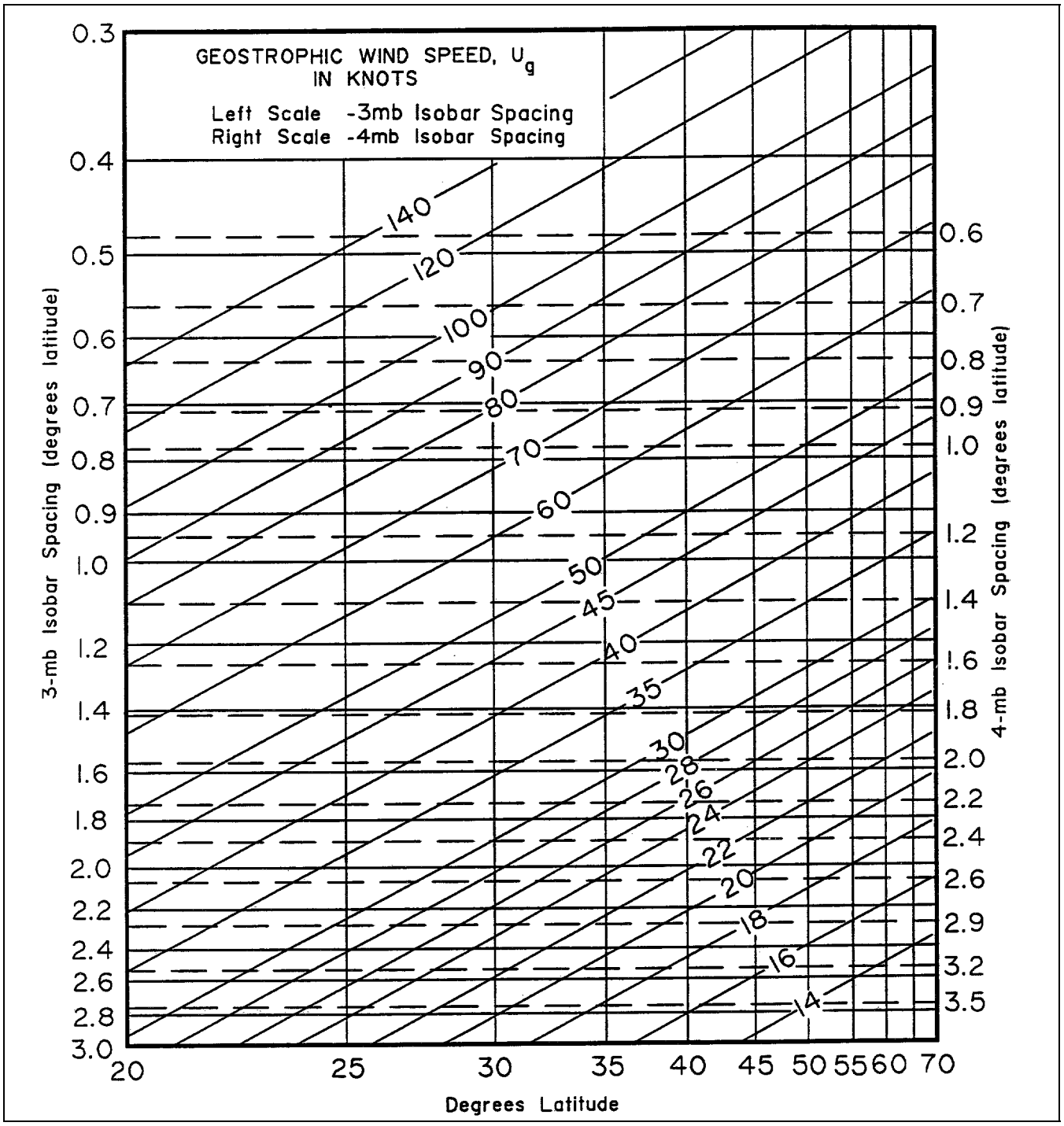

Figure 3-13. Geostrophic wind scale

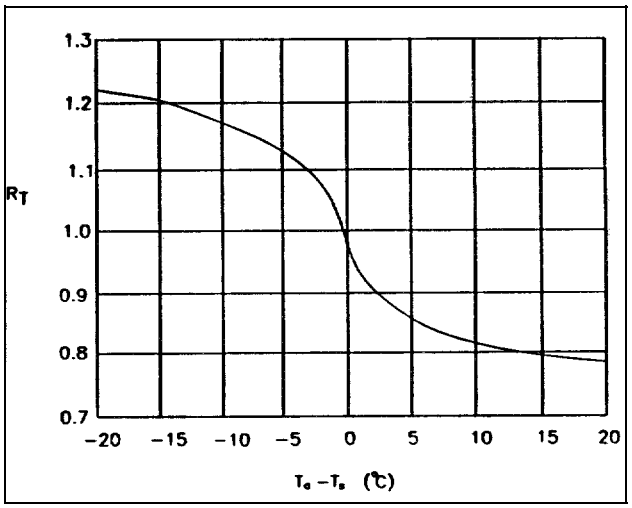

Figure 3-14. Correction factor for the air-sea temperature difference, (T_a - T_s)°C (after Resio and Vincent 1977)

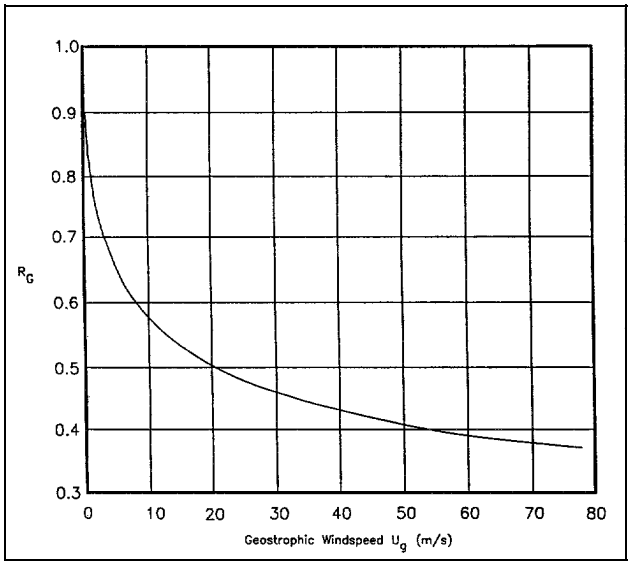

Figure 3-15. Correction factor to convert the geostrophic wind speed to the 10-meter elevation wind speed

********** EXAMPLE 3-2 **********

GIVEN: An examination of a series of synoptic charts indicated that the conditions in Figure 3-12 persisted for 10 hour. The air and sea temperature were reported at 9 °C and 11 °C, respectively.

FIND: Estimate the wave height and period generated by these weather conditions at approximately 54 °N 130 °W.

SOLUTION: This problem can be divided into four steps: delineate a fetch, calculate the geostrophic wind, calculate the wind stress, and estimate the wave conditions.

1) Fetch - The appropriate fetch for this location is fetch B in Figure 3-12. Noting that 5° latitude = 555 km (300 nmi), the fetch length is

F = 600 km (328 nmi)

2) Geostrophic Wind - The fetch width w and pressure change Δp are

w = 1.9 °lat
Δp = 12 mb

The isobar spacing s on this synoptic chart is

s = 4 mb

The pressure gradient across the fetch is

$$p_g = \frac{w(°\text{lat})}{\Delta p(mb)}\, s(mb) = \frac{1.9}{12}\, 4 = 0.63\ °\text{lat}$$

The center of the fetch is at 52 °N. Figure 3-13 gives

U_g = 75 knots = 38.6 m/sec

3) Wind Stress - The air-sea temperature difference is

$T_a - T_s$ = 9 - 11 = -2 °C

Figure 3-14 yields

R_T = 1.07

For U_g = 38.6 m/sec, Figure 3-14 gives

R_G = 0.44

The corrected wind speed is determined from Equation 3-5

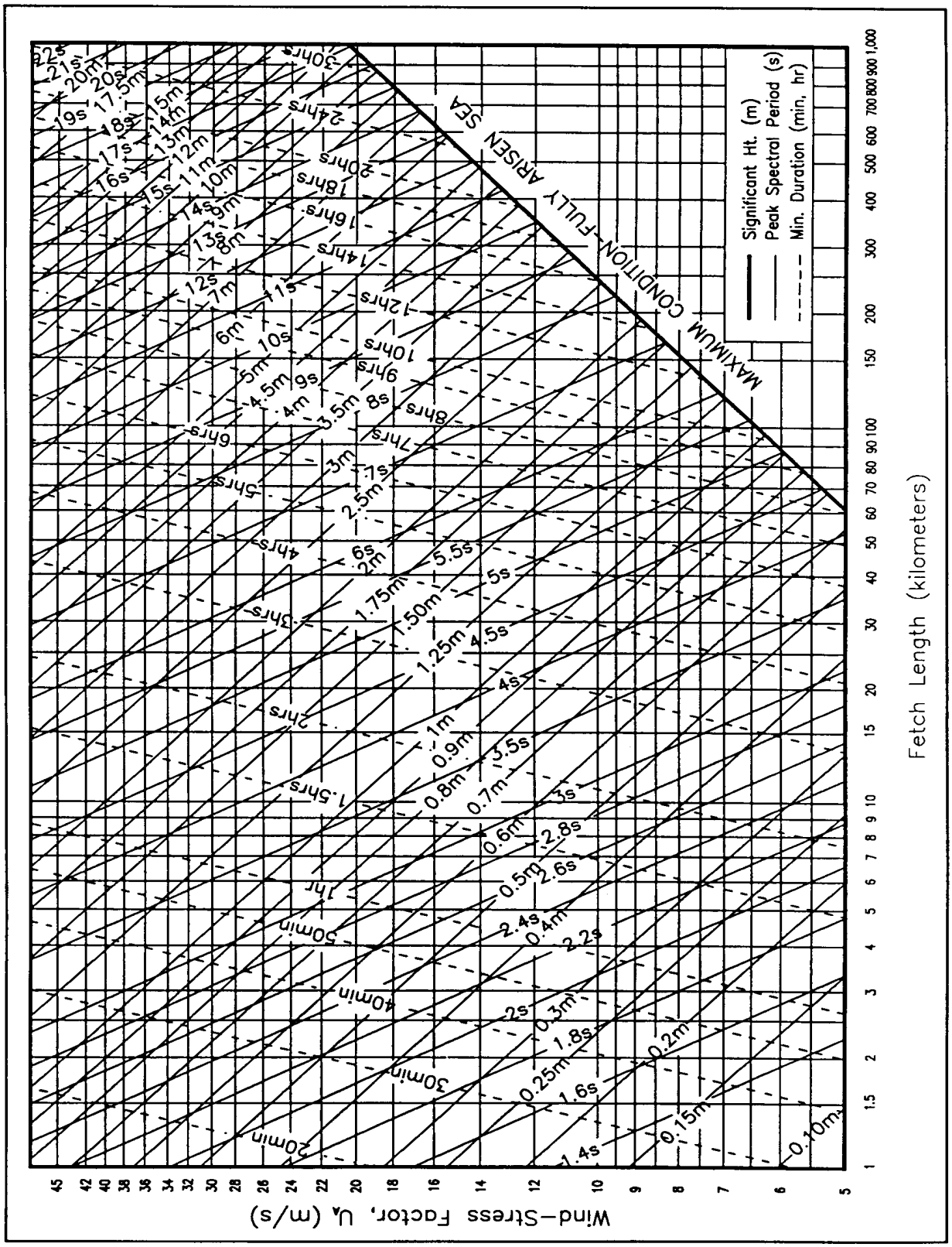

Figure 3-16. Nomograms of deepwater significant wave prediction as a function of the wind stress factor, fetch length, and wind duration

$U = R_T\, R_G\, U_g$ = (1.07)(0.44)(38.6) = 18.2 m/sec (59.7 ft/sec)

This is converted to a wind stress using Equation 3-6

$U_A = 0.71\, U^{1.23} = 0.71\, (18.2)^{1.23} = 25.2$ m/sec (82.7 ft/sec)

4) Wave Prediction - For U_A = 25.2 m/sec (82.7 ft/sec), F = 600 km (328 nmi) and t = 10 hours, the significant wave height and peak period are estimated from Figure 3-15.

H_s = 5.4 m (17.7 ft) T_p = 10.3 sec

********** END EXAMPLE 3-2 **********

3-5. Wave Transformations

As waves propagate from the deep water generation area to the design site, they undergo a number of transformations. The local waves in the generation area are referred to as seas. Local seas are typically steeper and short crested. As they propagate, they become more regular and transform into longer period, lower wave height swell. Long period waves propagate faster than short period waves. After traveling several thousand kilometers, this transformation yields a more peaked spectrum (narrow frequency range) for swell waves. Figure 3-17 may be used to estimate swell period as a function of travel distance. Use of these curves requires the wave period leaving the fetch, T_F (seconds), the minimum fetch, F_{min} (nmi), and the travel distance, D (nmi). In the case of a fetch limited storm, the minimum fetch corresponds to the actual fetch. For a duration limited storm, F_{min} corresponds to the fetch length at the duration limit. These curves should be used only as an indicator of wave period increase with travel distance.

********** EXAMPLE 3-3 **********

GIVEN: A storm with F_{min} = 740 km (400 nmi) generates waves with T_F = 10 s.

FIND: Estimate the swell conditions for a travel distance of 3700 km (2000 nmi).

SOLUTION: The conditions for this example are shown on Figure 3-17. The decayed wave period is

$T_D/T_F = 1.28$; T_D = 12.8 s

********** END EXAMPLE 3-3 **********

a. Nearshore. As the waves approach the shoreline, they will be modified by interactions with the bottom. These modifications are shoaling, refraction, diffraction, dissipation, and breaking. The local wave height H is given by

$$H = K_s\, K_R\, K_D\, K_F\, H_O \qquad (3\text{-}7)$$

where K_S is the shoaling coefficient, K_R is the refraction coefficient, K_D is the diffraction coefficient, K_F is the dissipation coefficient, and H_0 is the deep water wave height.

(1) Shoaling is the change in wave height required for the conservation of wave energy flux to balance the change in the group velocity as the waves enter shallower water. The linear wave theory shoaling coefficient K_s is given by

$$K_S = \tanh(kd)\left(1 + \frac{2kd}{\sinh(2kd)}\right)^{\frac{1}{2}} \qquad (3\text{-}8)$$

in which k is the wave number (= $2\pi/L$) . Tabulated values of the shoaling coefficient are given in Appendix C of the Shore Protection Manual (1984).

(2) Refraction is the bending of wave crests due to phase speed differences associated with different water depths. Refraction is a site specific wave transformation. If the bottom contours are straight and parallel, and the waves are normally incident to the shoreline, then no refraction occurs. If the contours are straight and parallel (this does not require a planar slope) and the waves approach at an angle, then analytical estimates of wave refraction are available. Combined refraction and shoaling coefficients for monochromatic waves are given in Figure 3-18 for straight and parallel bottom contours. Figure 3-18 also gives the angle of the wave crest to contour (local wave angle), α.

(3) Refraction of random seas depends on the peakedness of the spectrum. Even if the predominant wave direction is normal to the coastline, there will be refraction. This is due to the refraction of waves with directions other than the predominant direction. This effect decreases for narrow spectra. Refraction coefficients K_R for random seas on a coast with straight and parallel depth contours given a predominant deepwater

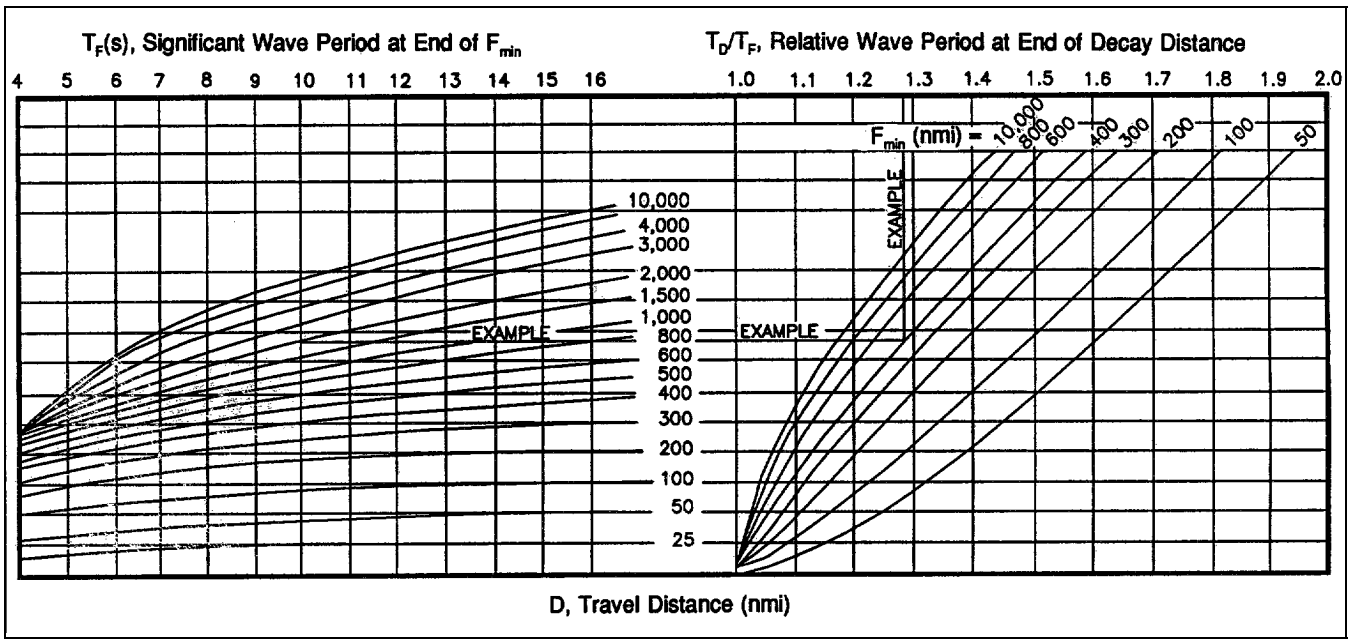

Figure 3-17. Wave period decay curves

direction $(\alpha_0)_P$ are given in Figure 3-19. The refraction angle of the predominant direction α_P is given in Figure 3-20. Several numerical shoaling and refraction models are listed in Appendix E.

(4) If the bottom contours cannot be approximated as straight and parallel, then graphical or numerical techniques must be employed to determine the refraction coefficient. The graphical template method is described in detail in the Shore Protection Manual (1984) in Chapter 2, Section III. This method may be used to construct wave rays to determine local refraction coefficients.

(5) Diffraction is the lateral transfer of wave energy due to variations in wave height along the crest. Diffraction is also a site specific wave transformation. Waves may be diffracted by surface piercing structures such as headlands, jetties, and breakwaters, or by bottom topography such as shoals and reefs. If these types of features exist near the design site, then diffraction effects must be considered. Graphical results for diffraction around the end of surface piercing structures are presented in the Shore Protection Manual (1984) for monochromatic waves and constant depth (Chapter 2). Similar graphs for random seas are presented in Chapter 7.

(6) Models of combined refraction and diffraction have been developed based on the parabolic equation method (Berkoff 1972). A review of these models is given in Liu, et al. (1986). This approach is generally limited to mild bottom slopes. However, this method represents a significant improvement in the determination of nearshore waves. The computer model RCPWAVE is based on this formulation (Ebersole, Cialone, and Prater 1986) (see Appendix E for a brief description). These combined refraction-diffraction models are not routinely employed on smaller projects.

(7) Dissipation is the loss of wave energy as the waves propagate shoreward. This is the result of viscosity, turbulence, bottom friction, percolation in the bottom, and wave-induced motion of the seabed. The importance of this wave dissipation is site specific. Along the Pacific coast of the continental United States, where the continental shelf is narrow, this loss of wave energy tends to be rather small. On coastlines with wide continental shelves, this dissipation may be significant. Numerical wave propagation models, such as those used in the WIS program, can incorporate this effect.

(8) Wave breaking is one of the most important wave transformations in the determination of nearshore

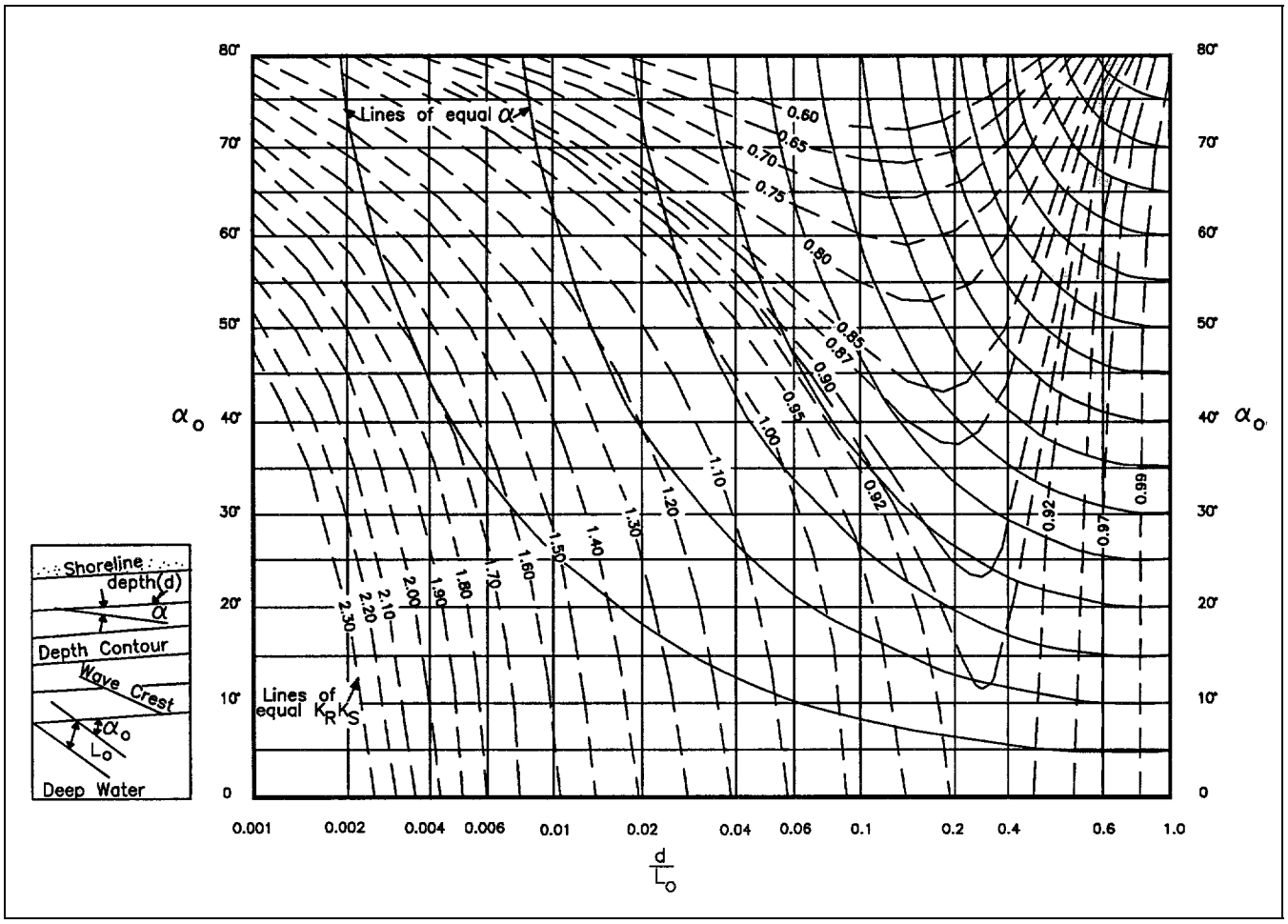

Figure 3-18. Change in monochromatic wave height and direction due to refraction and shoaling for straight and parallel bottom contours

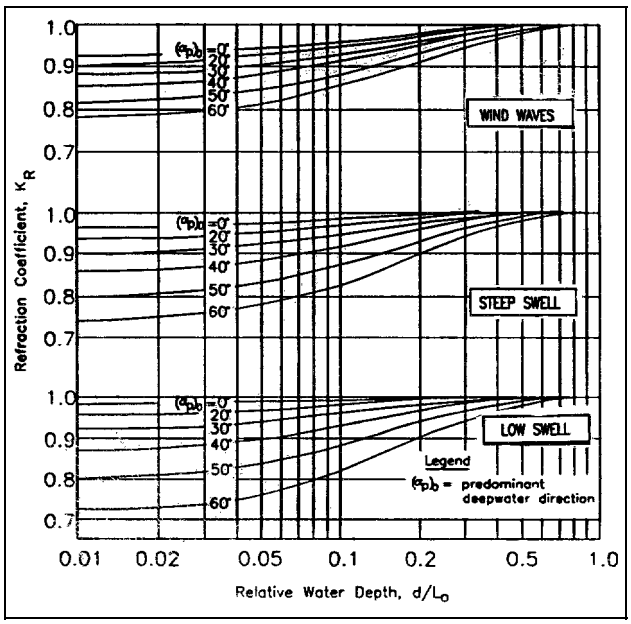

Figure 3-19. Refraction coefficients from random sea waves on a coast with straight and parallel bottom contours (Goda 1985)

currents and sediment transport. Unfortunately, wave breaking is not well understood. Models developed from the work of Longuet-Higgins and Cokelet (1976) show promise for quantifying the kinematics in near-breaking waves. However, these models have not evolved to a level that they can be used in routine design. Other models have been developed on the basis of momentum or energy flux (Peregrine and Svendsen 1978; Thornton and Guza 1983; Dally, Dean, and Dalrymple 1984). The Dally model is incorporated in RCPWAVE.

(9) The use of empirical curves remains a common method for estimating breaking wave conditions. Figures 3-21 and 3-22 provide a means of estimating the breaking wave height H_b and breaking depth d_b as a function of the wave steepness H_0'/L_0, where H_0' is the unrefracted deepwater wave height, and bottom slope m. Since refraction is site specific, this is a contrived method to remove this dependency. The deep water wave is shoaled and refracted onshore. It is then shoaled back out to sea without refraction to yield H_0'. This procedure enables curves for nearshore processes to be represented by the unrefracted deep water wave height.

(10) Breaking waves are often classified as spilling, plunging, or surging. Figure 3-21 shows the conditions for which these types of breakers occur. Profiles of these breaker types are given in Figure 3-23.

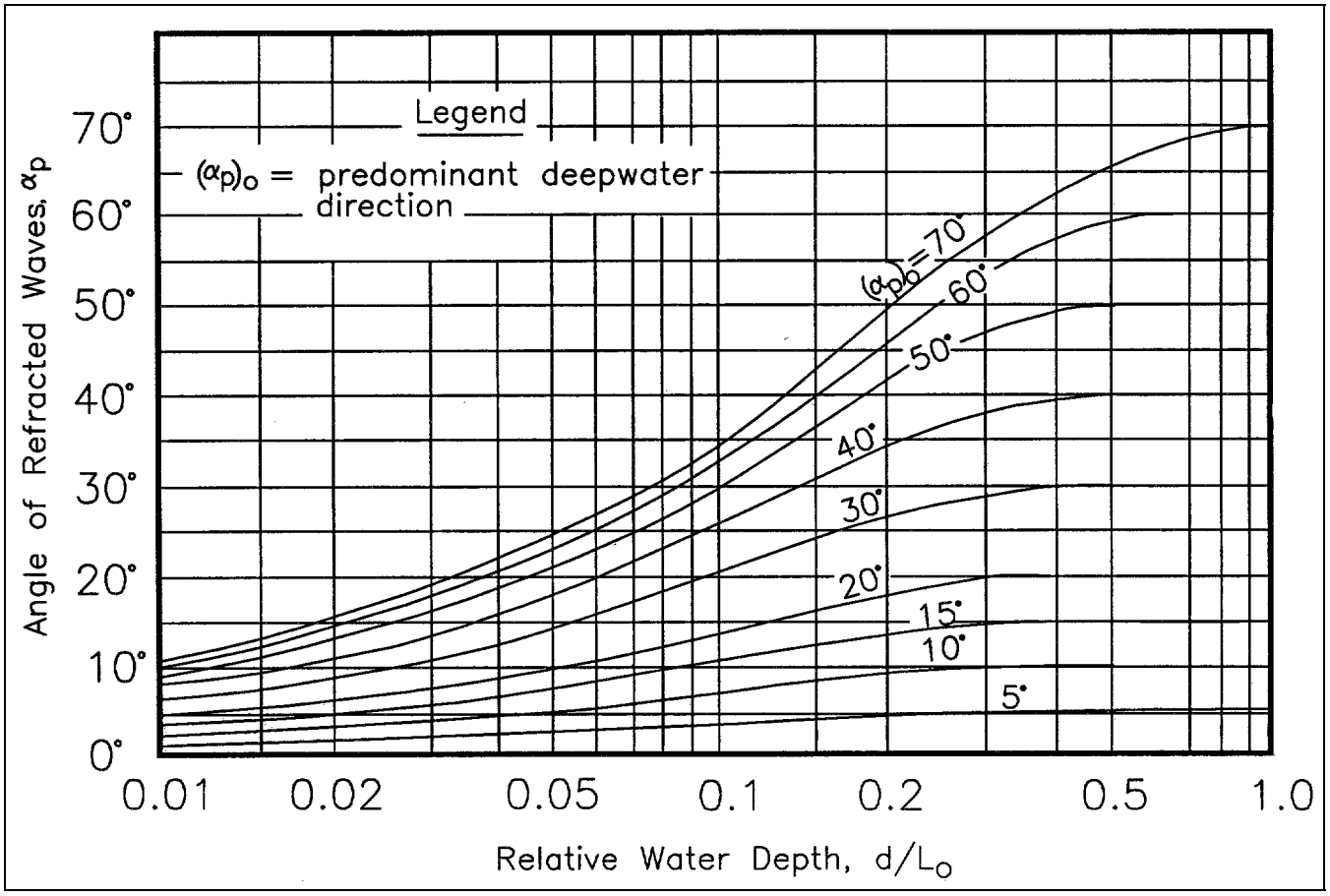

Figure 3-20. Variation of predominant wave direction for random sea waves on a coast with straight and parallel bottom contours (Goda 1985)

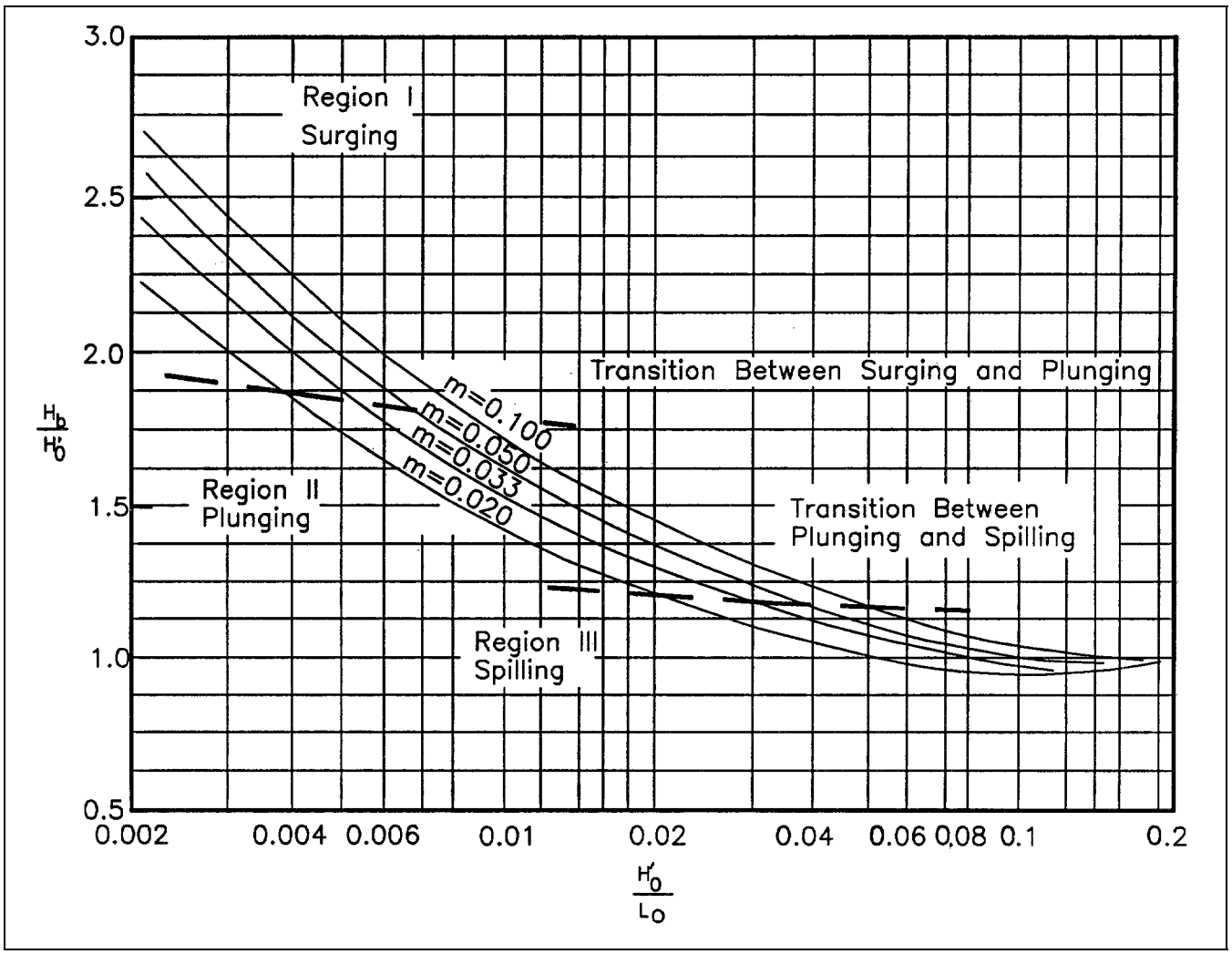

Figure 3-21. Breaker height dependency on wave steepness and bottom slope

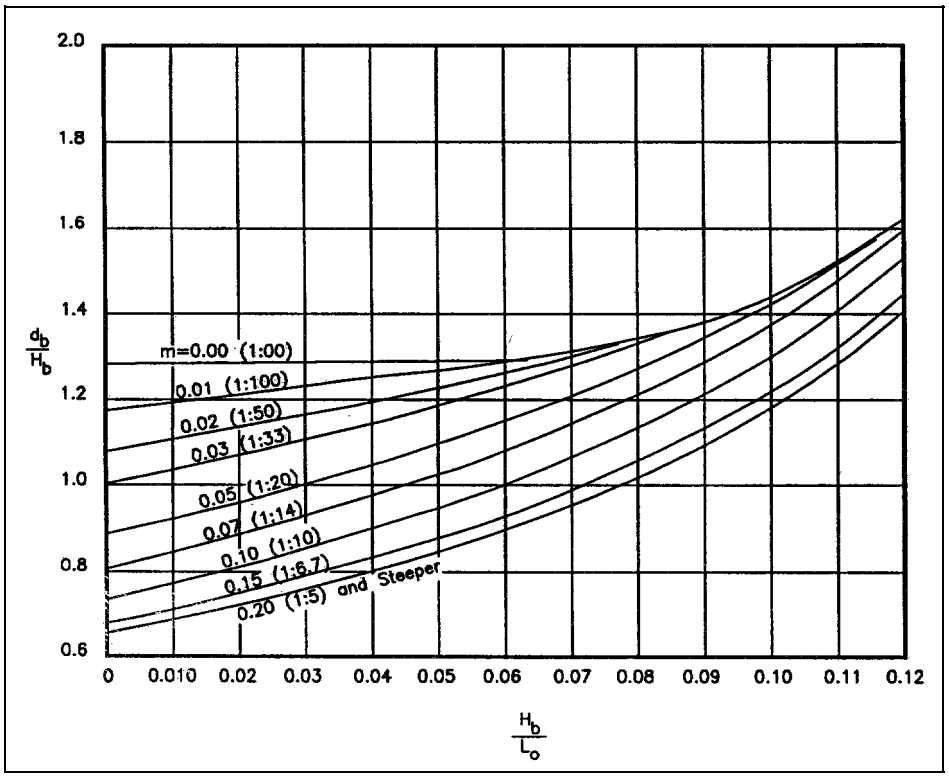

Figure 3-22. Breaker depth dependency on wave steepness and bottom slope

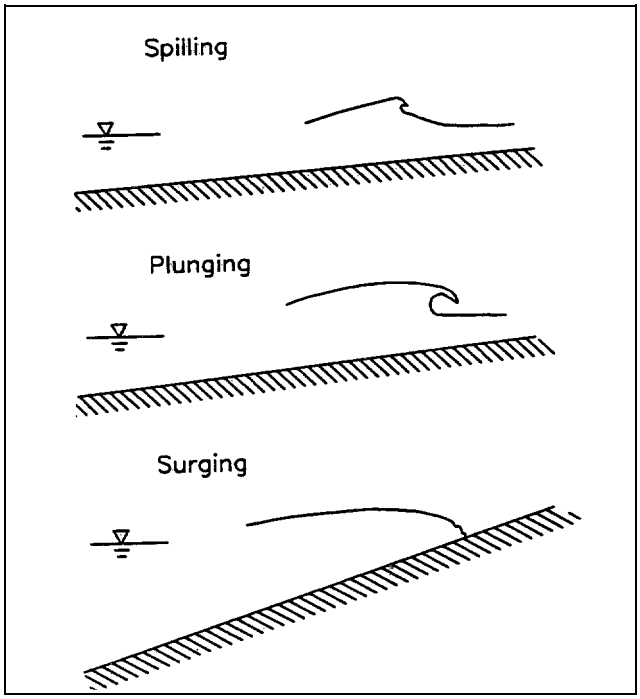

Figure 3-23. Breaking wave profiles